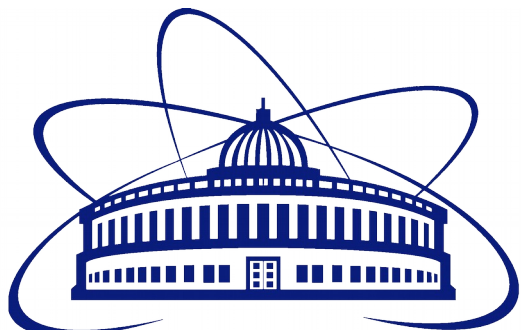


Progress in hyperon polarization analysis at NICA/MPD

Elizaveta Nazarova¹

**MPD Polarization Meeting
«Vorticity and Polarization in Heavy-
Ion Collisions»**

19.04.2022



¹ Joint Institute of Nuclear Research, Dubna, Russia



- Introduction
- Analysis technique
 - Simulation
 - Centrality determination
 - Event plane determination
 - Lambda reconstruction
 - Global polarization measurement
- Results
- Conclusions

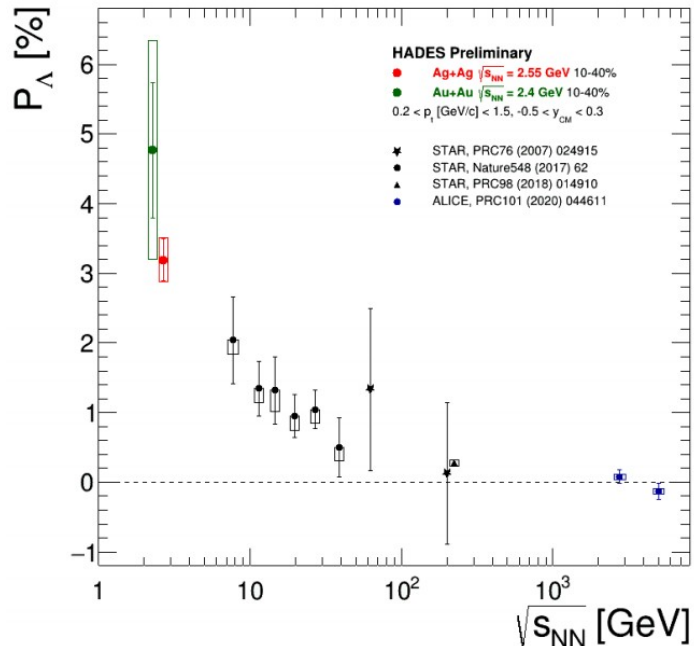
- Introduction
- Analysis technique
 - Simulation
 - Centrality determination
 - Event plane determination
 - Lambda reconstruction
 - Global polarization measurement
- Results
- Conclusions

Compared to the previous results

Introduction



- Predicted¹ and observed^{2,3} global polarization signals rise as the collision energy is reduced:
 - NICA energy range will provide new insight
- $\Lambda(\bar{\Lambda})$ - splitting of global polarization
- Comparison of models, detailed study of energy and kinematical dependences, improving precision
- Probing the vortical structure with new observables^{4,5}



¹ O. Rogachevsky, A. Sorin, O. Teryaev, Phys. Rev. C 82, 054910 (2010)

² J. Adam et al. (STAR Collaboration), Phys. Rev. C 98, 014910 (2018)

³ F. Kornas for the HADES Collaboration, SQM 2021

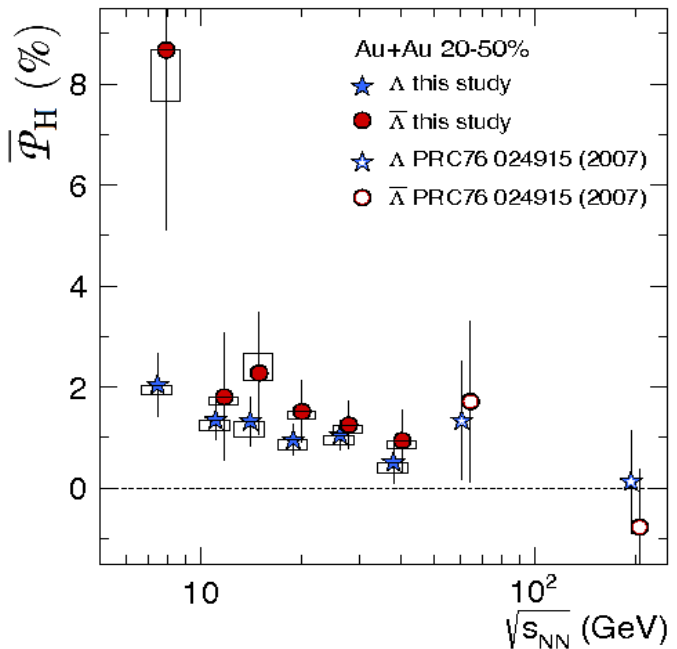
⁴ O. Teryaev and R. Usubov, Phys. Rev. C 92, 014906 (2015)

⁵ M. A. Lisa et al., Phys. Rev. C 104, 011901 (2021)

Introduction



- Predicted¹ and observed^{2,3} global polarization signals rise as the collision energy is reduced:
 - NICA energy range will provide new insight
- $\Lambda(\bar{\Lambda})$ - splitting of global polarization
- Comparison of models, detailed study of energy and kinematical dependences, improving precision
- Probing the vortical structure with new observables^{4,5}



¹ O. Rogachevsky, A. Sorin, O. Teryaev, Phys. Rev. C 82, 054910 (2010)

² J. Adam et al. (STAR Collaboration), Phys. Rev. C 98, 014910 (2018)

³ F. Kornas for the HADES Collaboration, SQM 2021

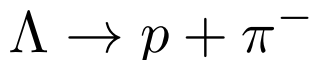
⁴ O. Teryaev and R. Usubov, Phys. Rev. C 92, 014906 (2015)

⁵ M. A. Lisa et al., Phys. Rev. C 104, 011901 (2021)

Global hyperon polarization



- w.r.t. reaction plane
- Emerges in HIC due to the system angular momentum^{1,2}
- Sensitive to parity-odd characteristics of QCD medium and QCD anomalous transport
- Measured through the weak decay:



$$\frac{dN}{d \cos \theta^*} = 1 + \alpha_H |\vec{P}_H| \cos \theta^*$$

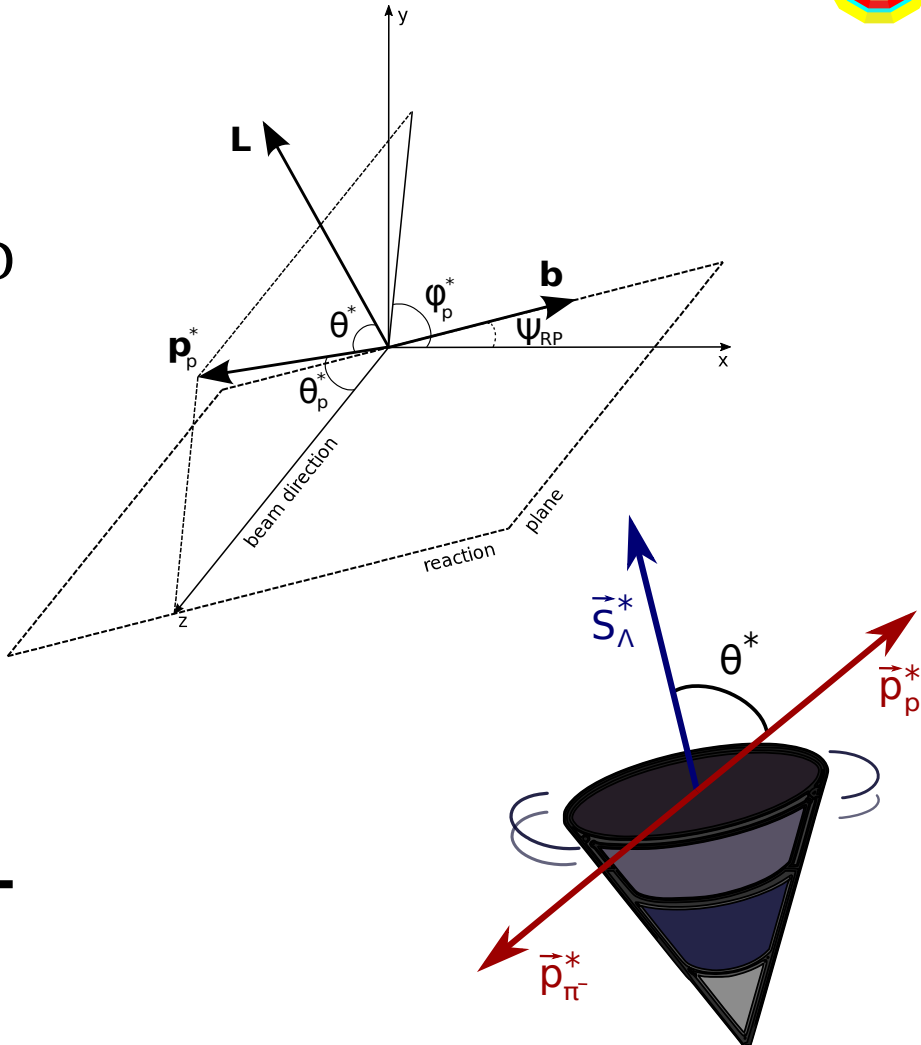
$$\alpha_\Lambda = -\alpha_{\bar{\Lambda}} \simeq 0.732 \text{ (Updated value³)}$$

- * — denotes hyperon rest frame (e.g. Λ)

¹ Z. Liang, X. Wang, PRL 94, 102301 (2005)

² L. Adamczyk et al., Nature 548, 62 (2017)

³ Ablikim M, et al., Nature Phys. 15:631 (2019)



Global hyperon polarization

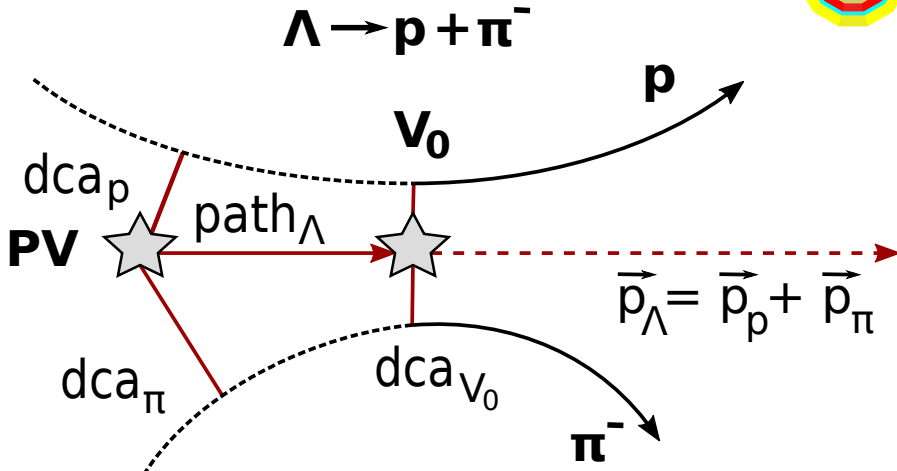


- θ^* — angle between the decay particle and polarization direction

$$\overline{P}_{\Lambda/\bar{\Lambda}} = \frac{8}{\pi\alpha} \frac{1}{R_{EP}^1} \langle \sin(\Psi_{EP}^1 - \phi^*) \rangle$$

- ϕ^* — azimuthal angle of decay particle

- Determine centrality
- Determine event plane (Ψ_{EP}^1, R_{EP}^1)
- Reconstruct Lambda
- Global polarization



- PV — primary vertex
- V_0 — vertex of hyperon decay
- dca — distance of closest approach
- path — decay length

MC
simulation
PHSD



Detector
simulation
GEANT 3



Event
reconstruction
MPD

- MC simulation using PHSD generator¹
 - Bi-Bi @ 9GeV, 10M MB events, b [0,12]fm (**request 23**)
 - Global hyperon polarization
 - Thermodynamical (Becattini) approach²

¹ W. Cassing, E. Bratkovskaya, PRC 78 (2008) 034919; NPA831 (2009) 215; W. Cassing, EPJ ST 168 (2009) 3

² F. Becattini, V. Chandra, L. Del Zanna, E. Grossi, Ann. Phys. 338 (2013) 32

MC
simulation
PHSD

- MC simulation using PHSD generator¹ (new)
 - Bi-Bi @ 9GeV, 10M MB events, b [0,12]fm (**request 23**)
 - Global hyperon polarization
 - Thermodynamical (Becattini) approach²

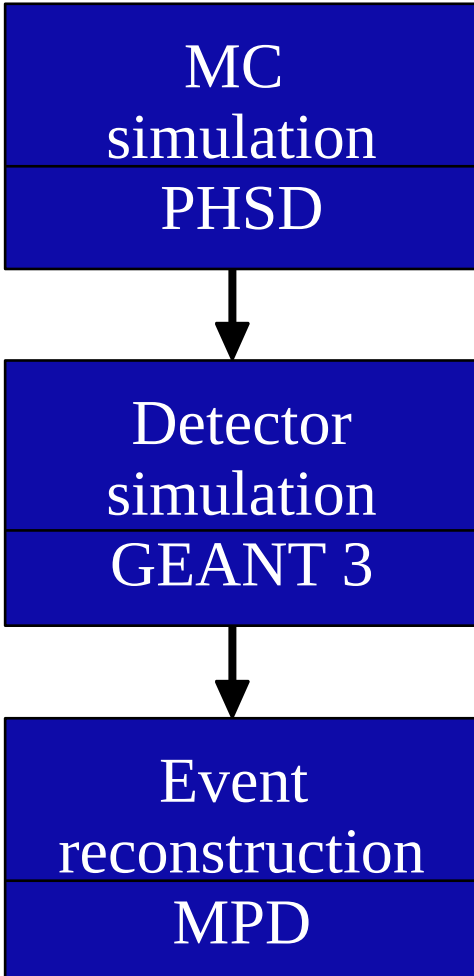
Detector
simulation
GEANT 3

- MC simulation using PHSD generator¹ (previous)
 - Au-Au @ 7.7GeV, 1.4M MB events, b [0,16]fm
 - Global hyperon polarization
 - Thermodynamical (Becattini) approach²

Event
reconstruction
MPD

¹ W. Cassing, E. Bratkovskaya, PRC 78 (2008) 034919; NPA831 (2009) 215; W. Cassing, EPJ ST 168 (2009) 3

² F. Becattini, V. Chandra, L. Del Zanna, E. Grossi, Ann. Phys. 338 (2013) 32



- Detector simulation
 - Transfer of hyperon polarization vector $\mathbf{P} = \{P_x, P_y, P_z\}$ from generator data (PHSD) to MCTracks
 - Accounts for non-unitary length of the vector (weight)
 - Polarization set to zero $\mathbf{P} = \{0,0,0\}$ if $P_n > 1$ (calculation of thermal vorticity is unreliable)
- Transfer of polarization during hyperon decays¹ (feed-down)
 - $\mathbf{S}_D^* = C \mathbf{S}_P^*$
 - D — daughter, P — parent, C — coefficient²
- Anisotropic decay of Λ hyperons (can be turned on/off)
 - $$\frac{dN}{d \cos \theta^*} = 1 + \alpha_\Lambda |\vec{P}_\Lambda| \cos \theta^* \quad (\text{recall})$$

¹ $\Xi^+(\Xi^-)$, Ξ^0 , Σ^0 decays ($C_{\Xi^-} = 0.927$, $C_{\Xi} = 0.9$, $C_{\Sigma} = -1/3$)

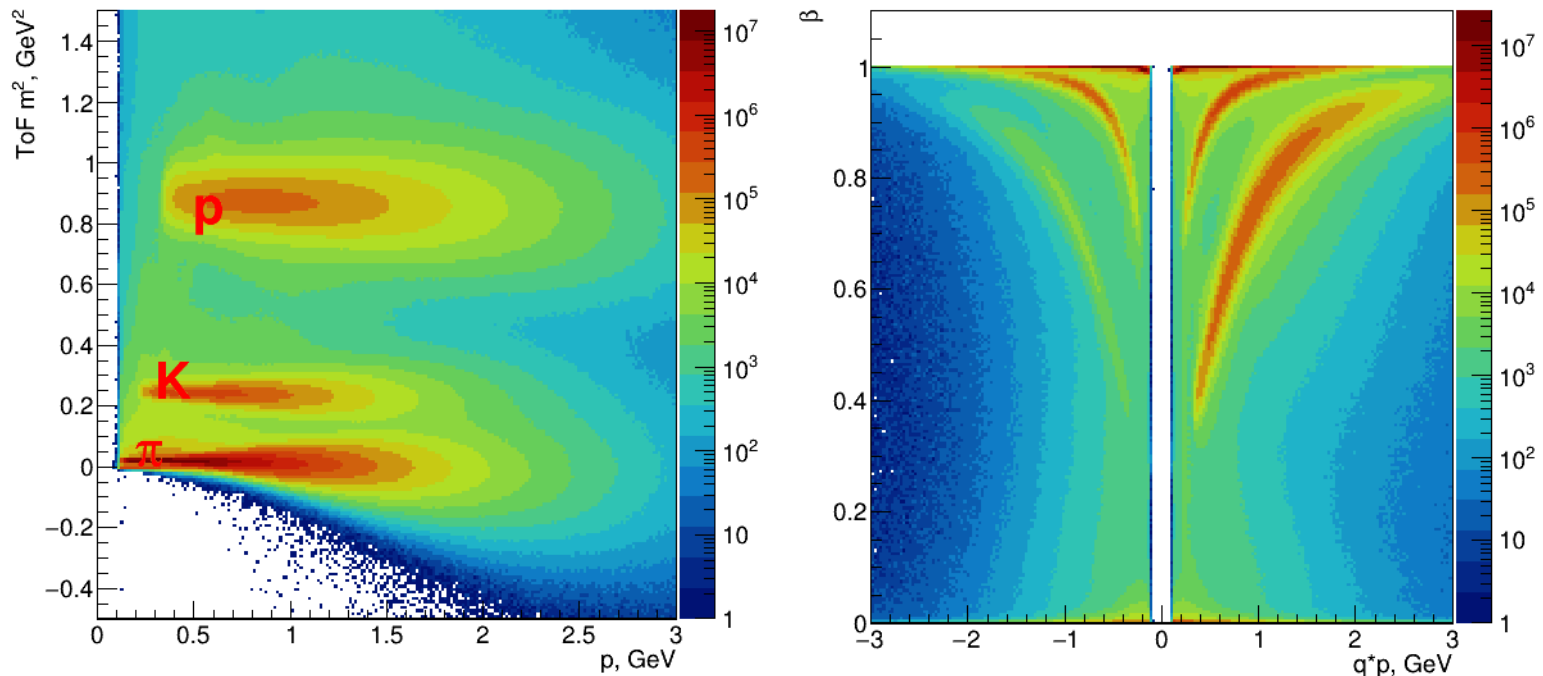
² F. Becattini et al., Phys.Rev.C 95 (2017) 5, 054902

MC
simulation
PHSD

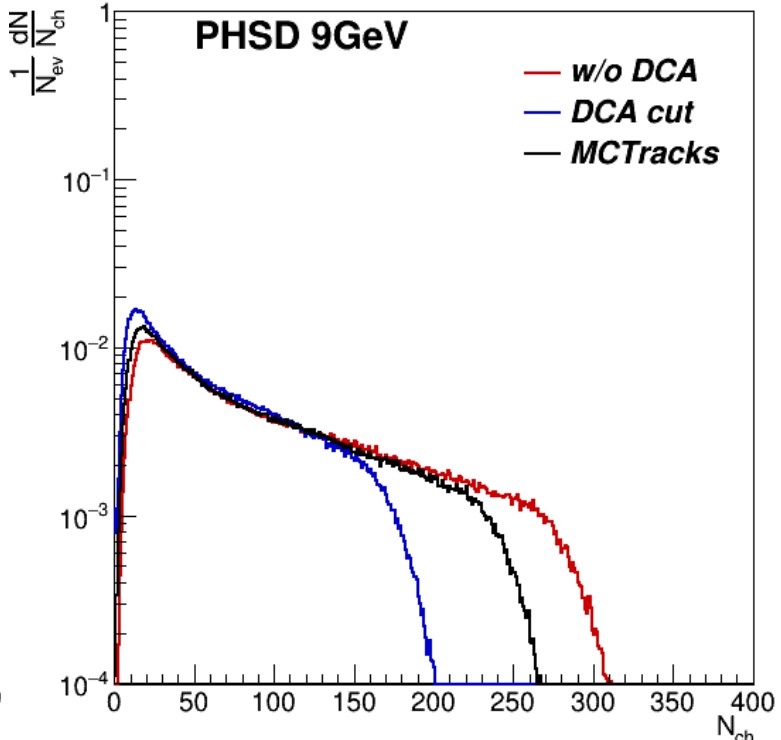
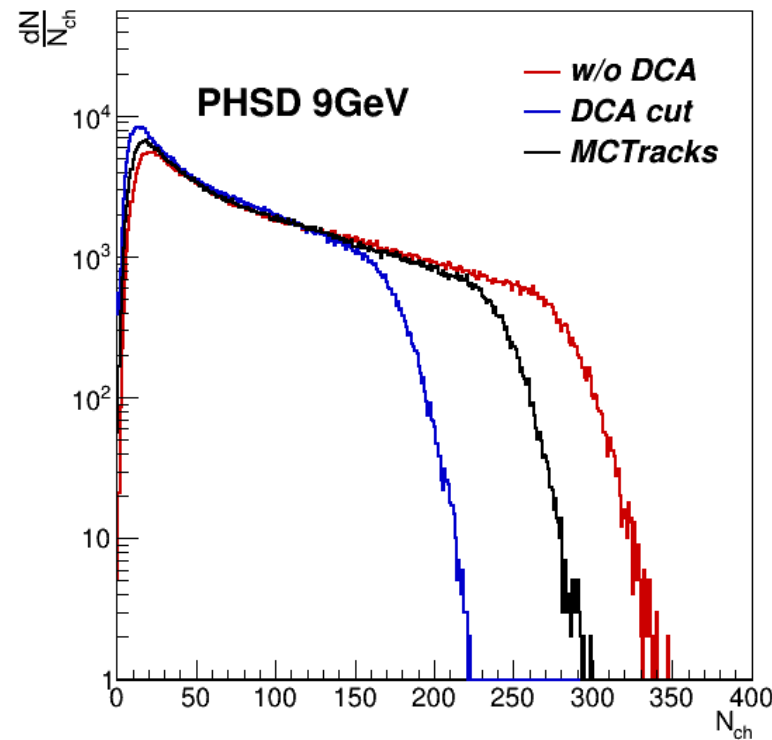
Detector
simulation
GEANT 3

Event
reconstruction
MPD

- Event reconstruction
 - Centrality and Event Plane determination
 - Realistic PID
 - Reconstruction of Λ hyperons via their weak decay



Centrality determination



- MC-Glauber based centrality framework¹
- Selection criteria:
 - > 500k events
 - > $|\eta| < 0.5$
 - > $|p_T| > 0.15$ GeV
 - > $N_{\text{hits}} > 16$
 - > $|DCA| < 0.5$ cm (optional)
 - > 10%-centrality bins

¹ P. Parfenov et al, NRNU MEPhI for the MPD collaboration
(<https://github.com/FlowNICA/CentralityFramework>)

DCA comparison in Back-Up

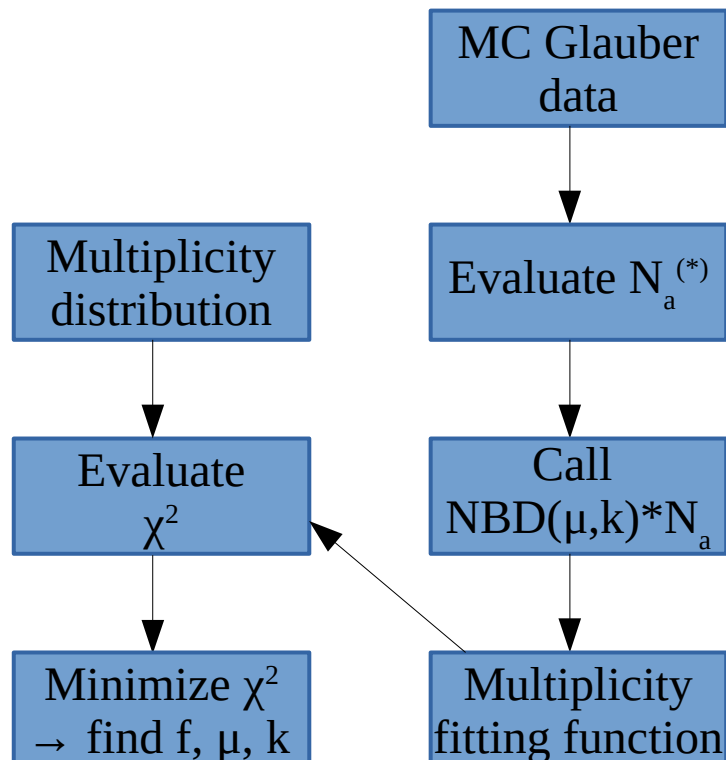
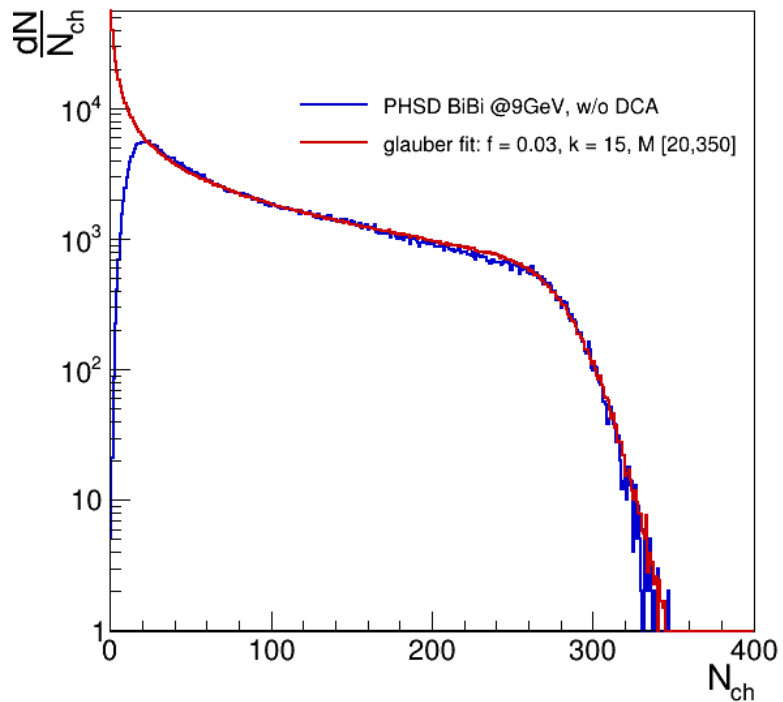
Centrality determination



- MC-Glauber based centrality framework¹

- Selection criteria:

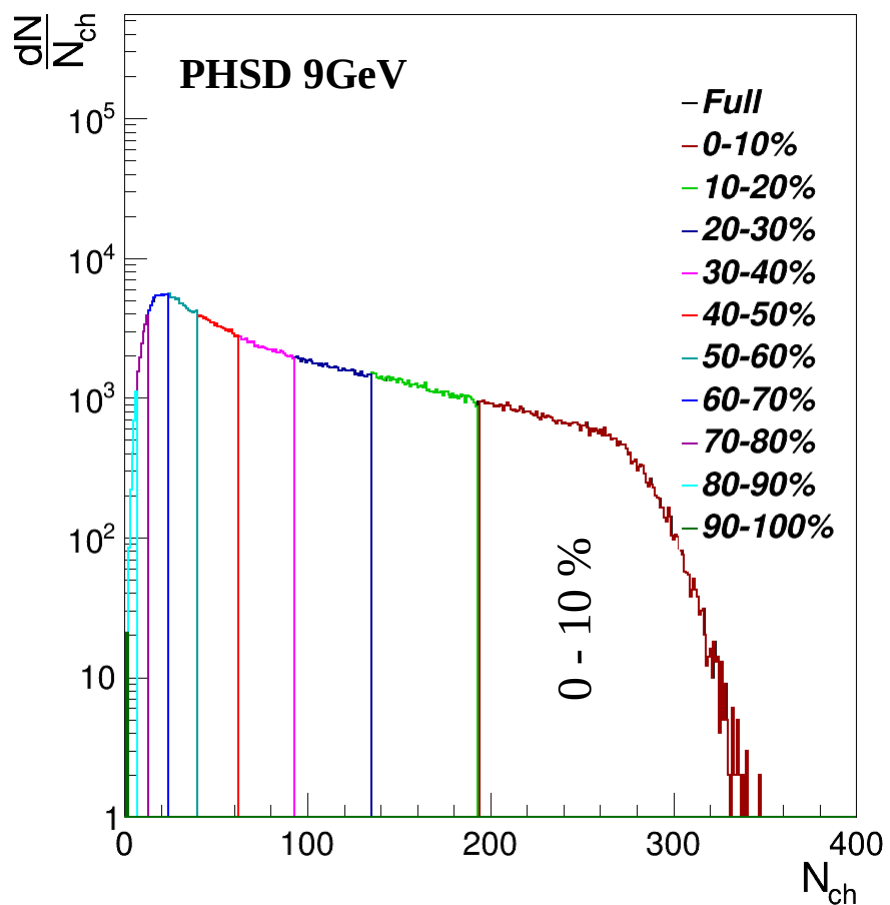
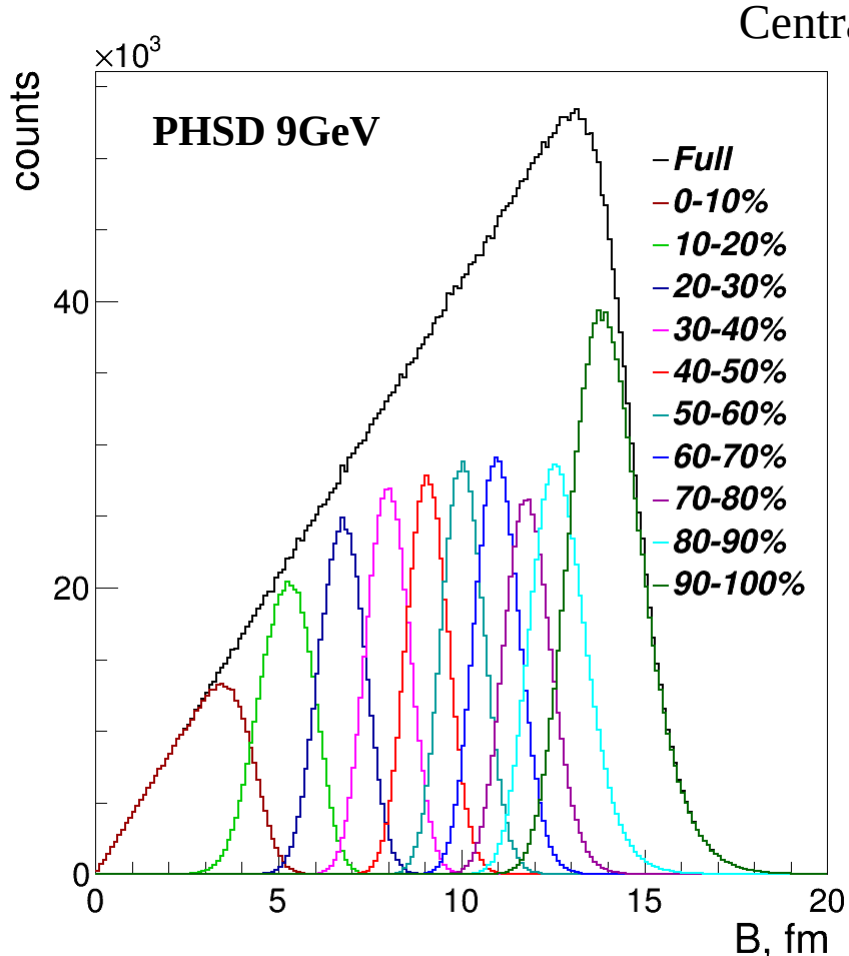
- 500k events
- $|\eta| < 0.5$
- $|\mathbf{p}_T| > 0.15 \text{ GeV}$
- $N_{\text{hits}} > 16$
- 10%-centrality bins



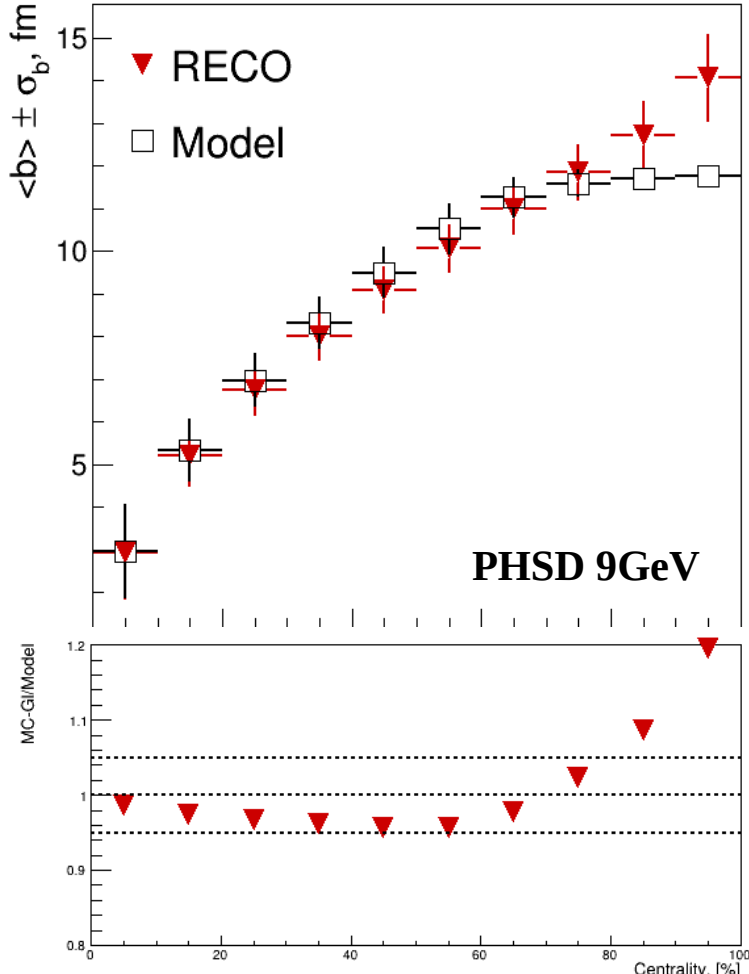
¹ P. Parfenov et al, NRNU MEPhI for the MPD collaboration (<https://github.com/FlowNICA/CentralityFramework>)

$${}^{(*)}N_a = fN_{\text{part}} + (1 - f)N_{\text{coll}}$$

Centrality determination



Centrality determination



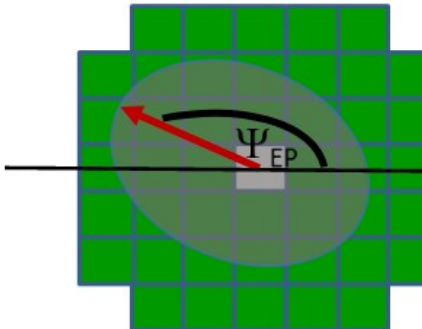
- Completed calibration of centrality
 - Full analysis done for 10%-centrality bins
 - 4 intervals of centrality chosen for analysis (0-10%, 10-20%, 20-50%, 50-100%), for comparison with previous results
- Choice of b [0,12]fm reduces amount of events without interaction (~1% compared to ~20% we had with b [0,16]fm)
- Agreement within ~5% for impact parameter
 - Except for the last two centrality bins (80-90%, 90-100%)
 - Excluded them from the main analysis

Event plane determination



- Event plane angle can be measured as:

- $\Psi_{\text{EP}}^n = \frac{1}{n} \arctan \frac{Q_y}{Q_x}$
- $Q_y = \sum_i w_i \sin(n\phi_i)$
- $Q_x = \sum_i w_i \cos(n\phi_i)$



$$w_i = E_i/E_{\text{total}} \text{ (FHCal)}$$

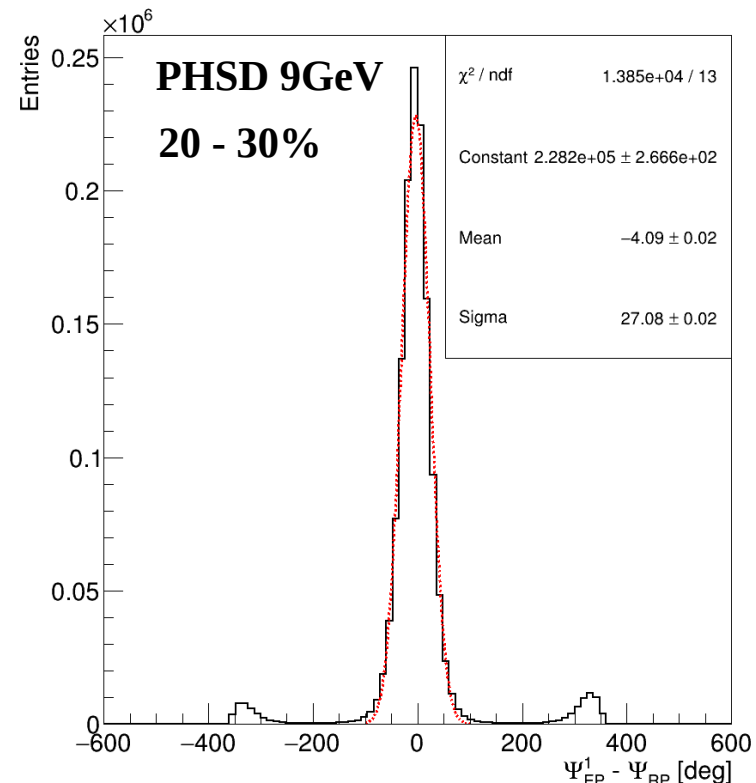
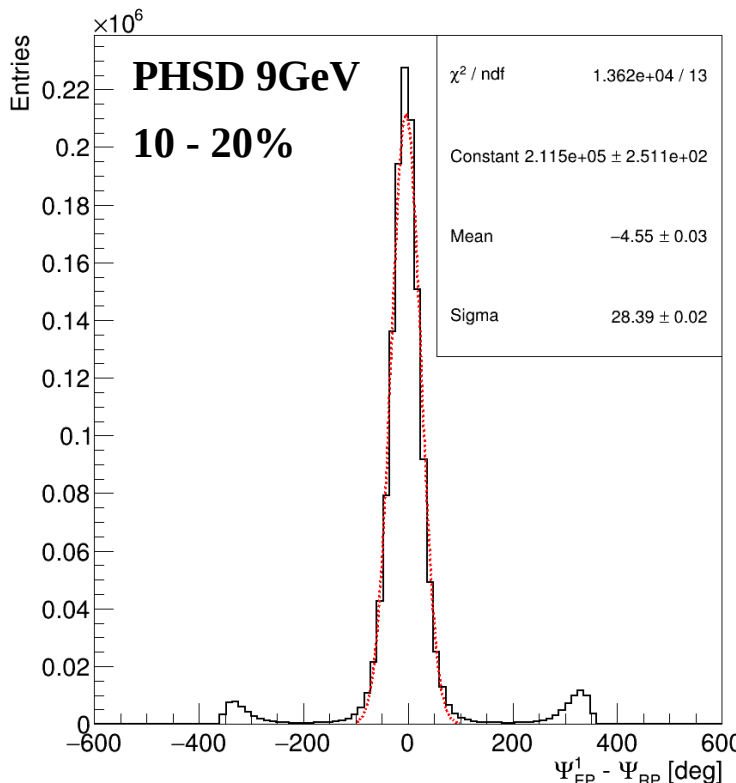
$$w_i = p_{T,i}/p_{T,\text{total}} \text{ (TPC)}$$

- Event plane resolution can be calculated as:

- $R_{\text{EP}}^k = \langle \cos(k(\Psi_{\text{EP}}^n - \Psi_{\text{RP}})) \rangle$ (w.r.t. reaction plane angle from the model)
- $R_{\text{EP}}^k = \sqrt{\langle \cos(k(\Psi_{\text{EP,R}}^n - \Psi_{\text{EP,L}}^n)) \rangle}$ (sub-event resolution method¹)

¹ A. M. Poskanzer , S. Voloshin Phys.Rev. C (1998) 58. pp. 1671–1678

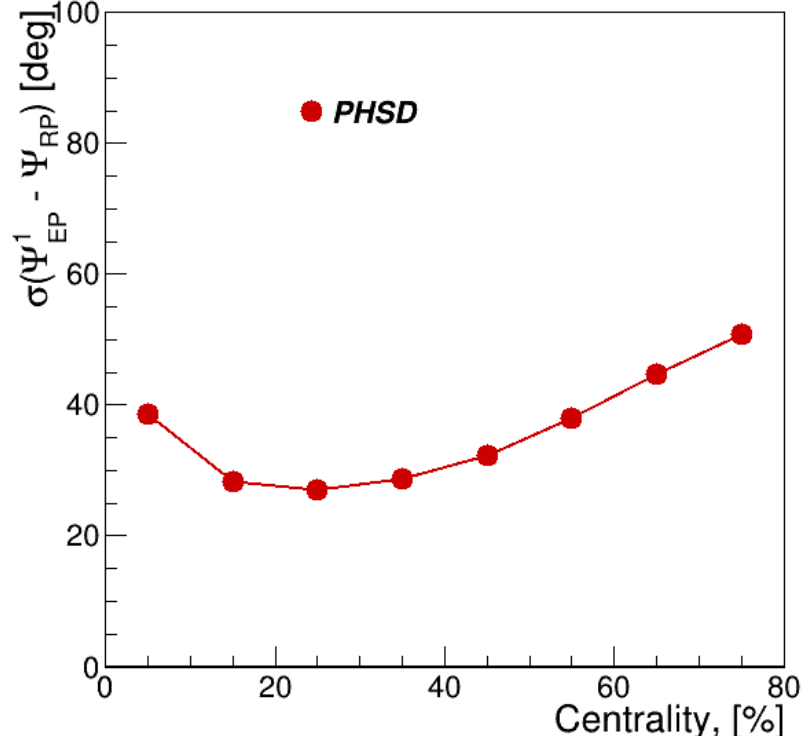
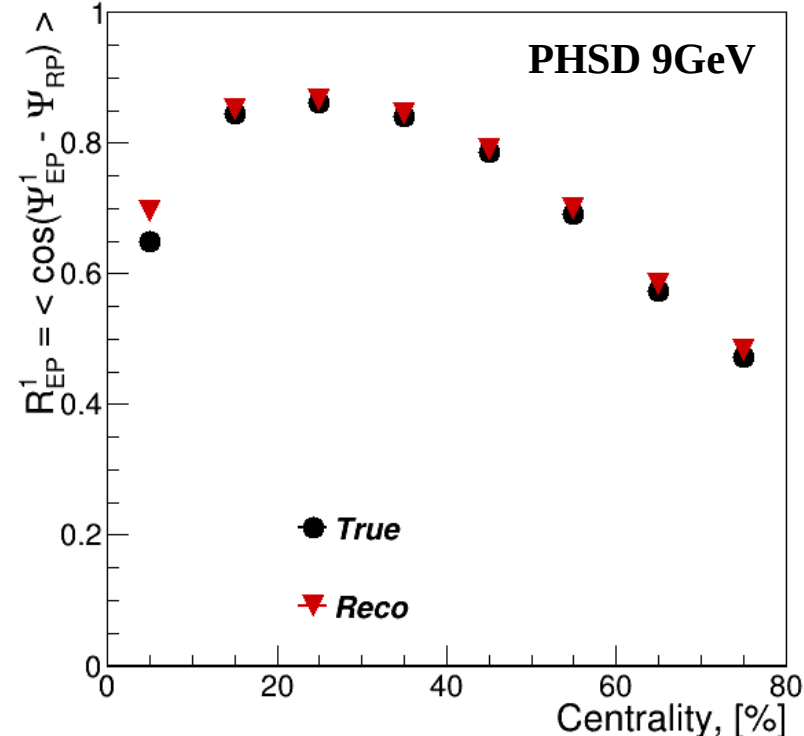
Event plane determination



- ➊ Difference between EP and RP angles
 - Gaussian fit
 - Max. resolution of ~ 27 deg.
 - Centered at 0

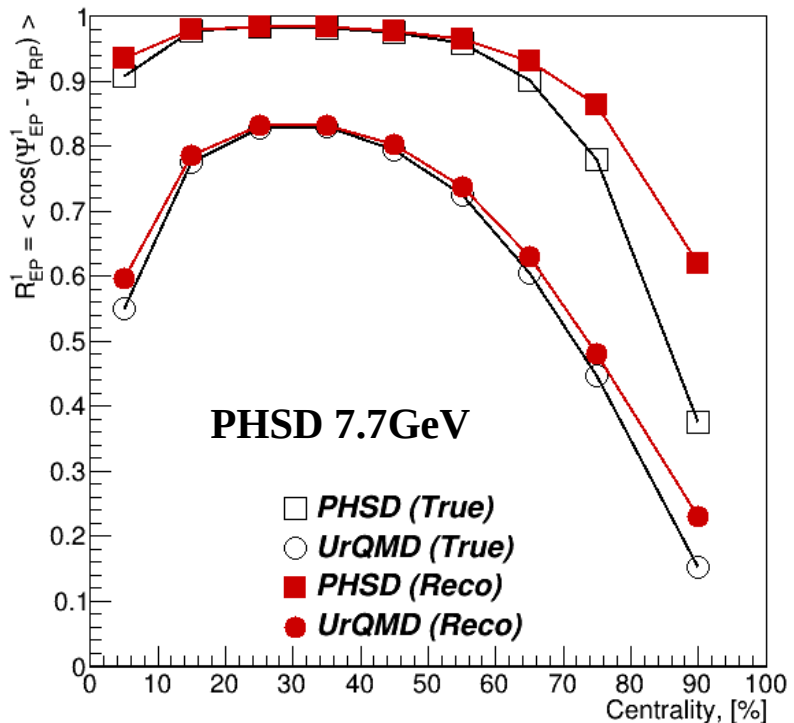
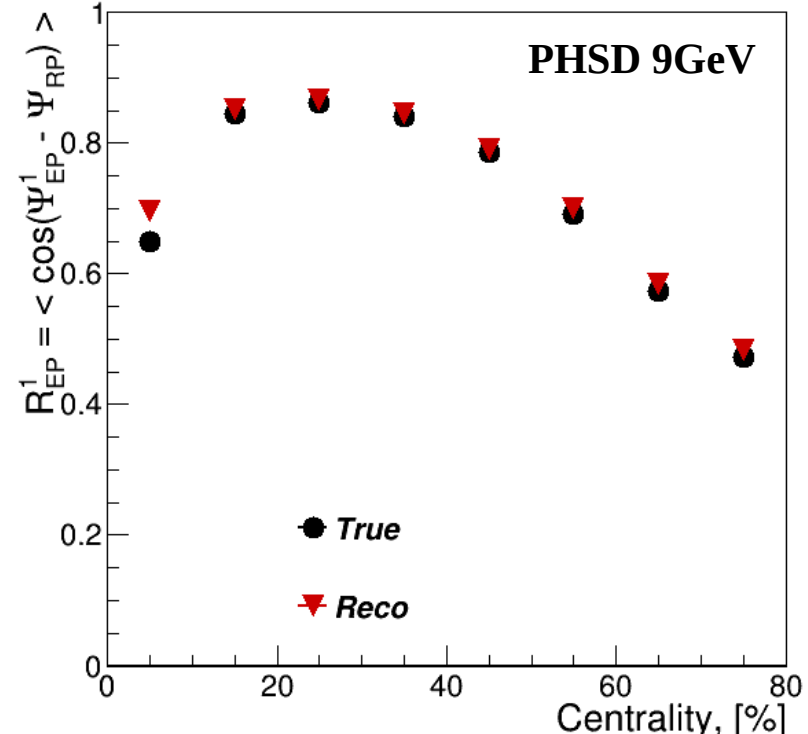
$$R_{\text{EP}}^k(\text{sub}) = \frac{\sqrt{\pi}}{2\sqrt{2}} \chi \exp(-\chi^2/4) [I_{(k-1)/2}(\chi^2/4) + I_{(k+1)/2}(\chi^2/4)]$$

Event plane determination



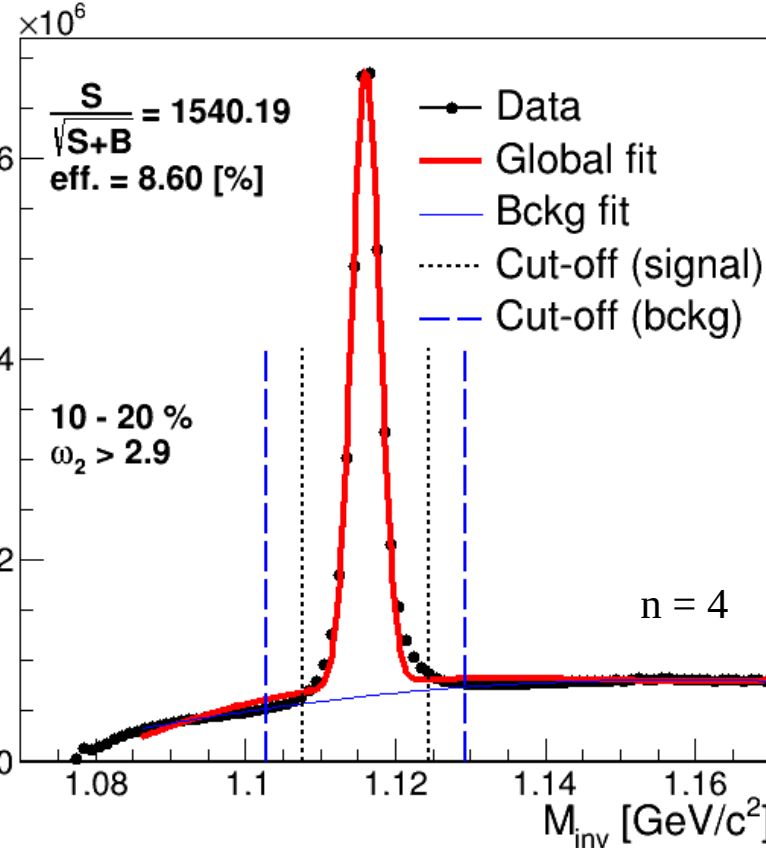
- Event plane and its resolution determined using FHCAL
- Checked via 2 methods

Event plane determination



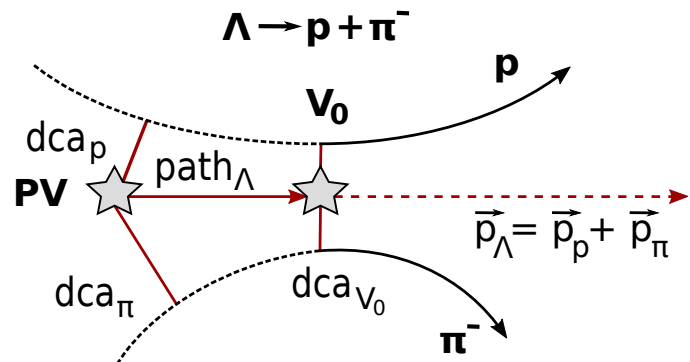
- Event plane and its resolution determined using FHCAL
- Reasonable behaviour compared to the previous results

Lambda reconstruction



Fitting procedure:

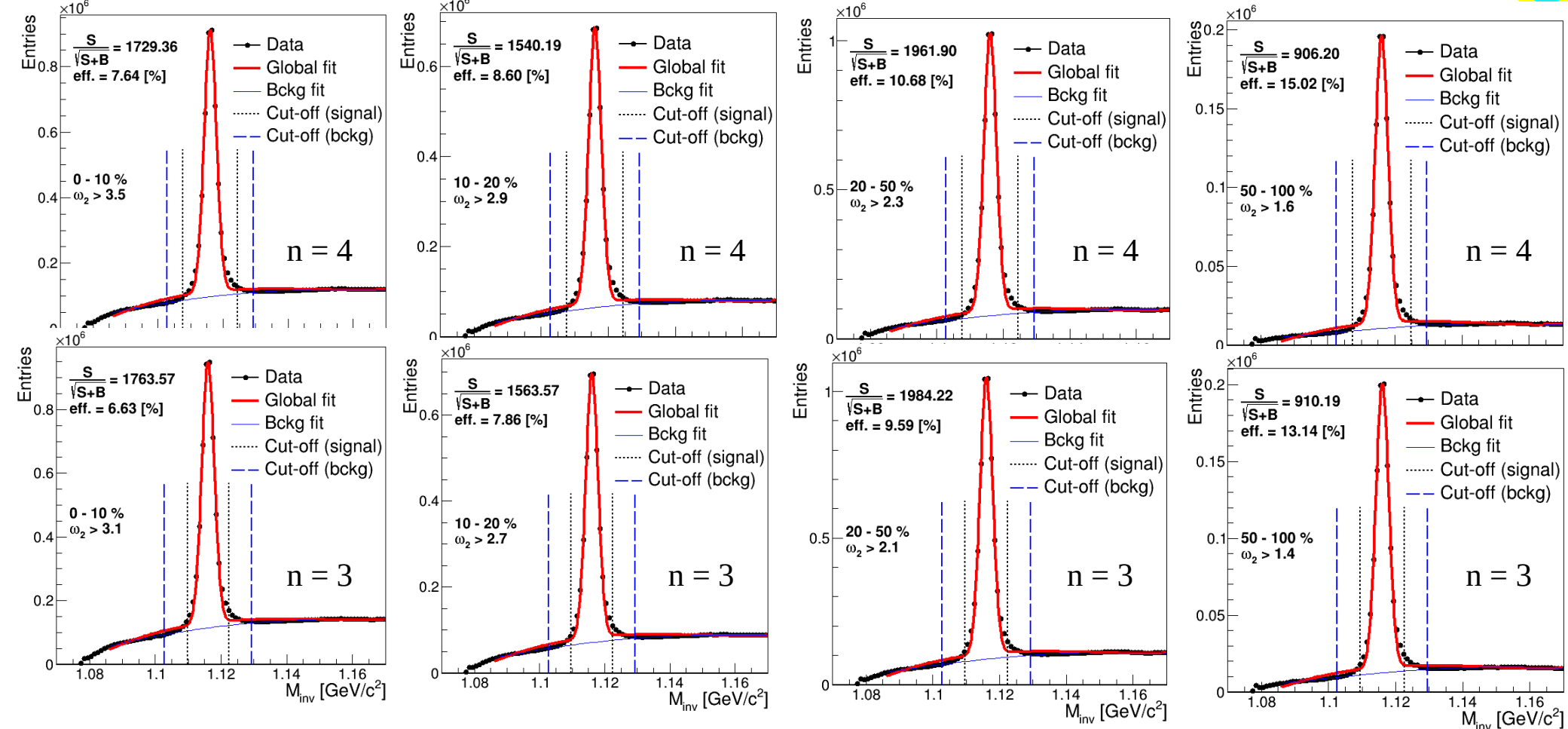
- Global fit (Gauss + Legendre polynomials)
- Background fit in sidebands ($\pm 7\sigma$)
- Cut-off: $\langle M_\Lambda \rangle \pm n^* \sigma$
- ω_2 cut based on maximum significance (for each centrality bin)



$$\omega_2 = \ln \frac{\sqrt{\chi_\pi^2 \chi_p^2}}{\chi_\Lambda^2 + \chi_{V_0}^2}$$

$$f(x) = p_0 \exp \left(\frac{(-0.5(x - p_1))^2}{p_2^2} \right) + p_3(L_0 + p_4L_1 + p_5L_2 + p_6L_3 + p_7L_4)$$

Lambda reconstruction



Global polarization reconstruction

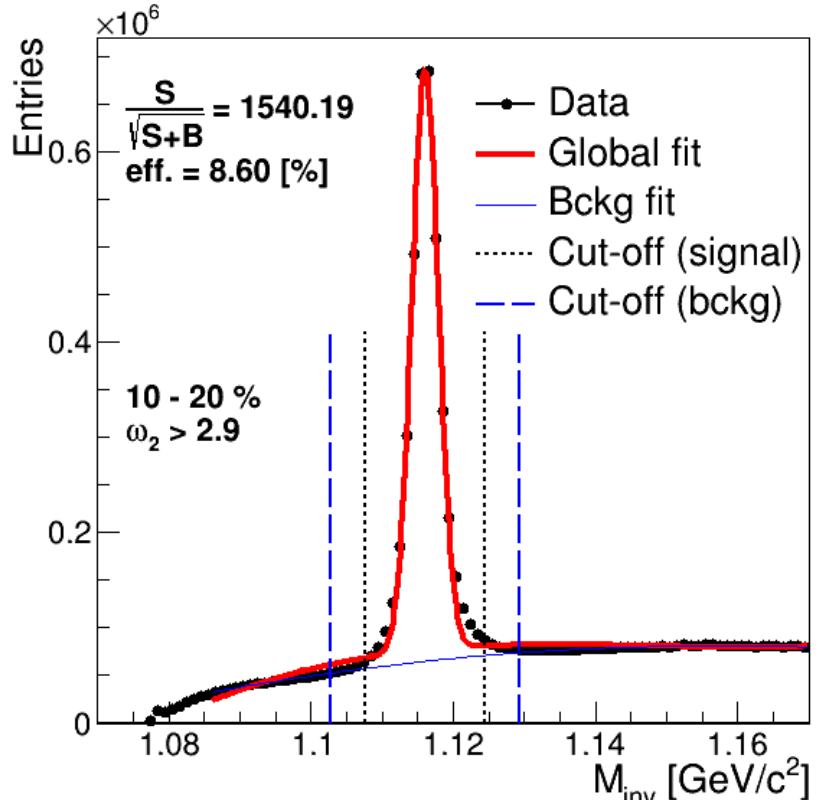


- Obtained invariant mass distribution in bins of $\Delta\phi_p^* = \Psi_{\text{EP}}^1 - \phi_p^*$
 - › Net amount of Λ in each bin
 - › Distribution of $N_\Lambda(\Delta\phi_p^*)$
- Fit of the distribution¹ to get $\langle \sin(\Delta\phi_p^*) \rangle \rightarrow P_\Lambda$
 - › «Event plane» method (p_n — fit parameters)
 - › $P_\Lambda = \frac{8}{\pi\alpha_\Lambda} \frac{p_1}{R_{\text{EP}}^1}$

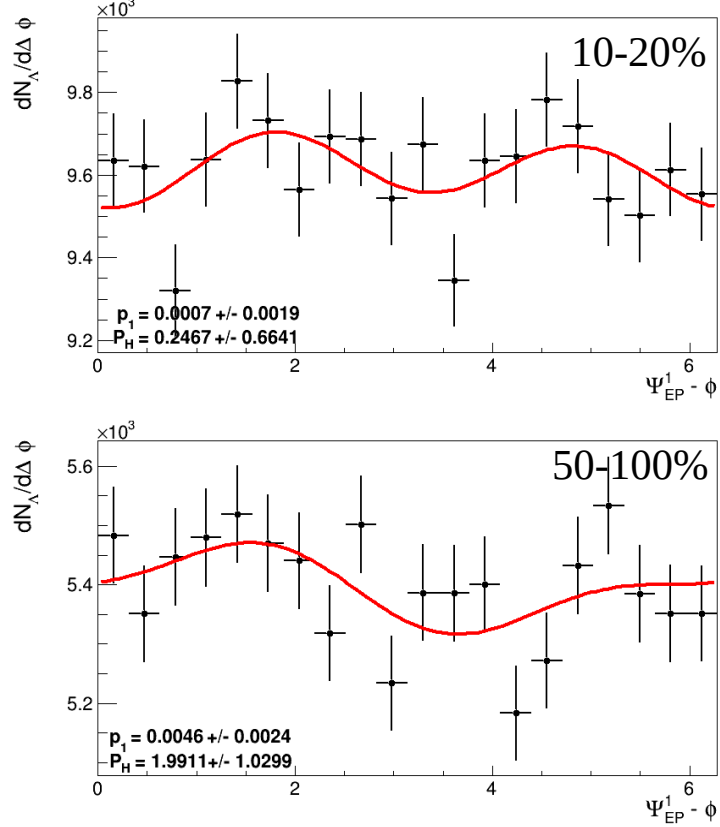
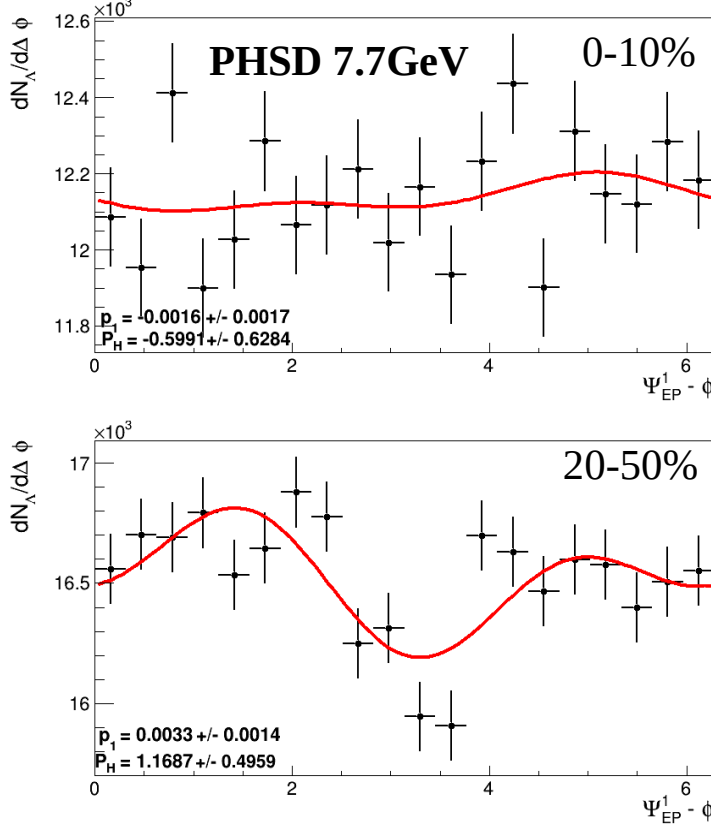
$$\overline{P}_{\Lambda/\bar{\Lambda}} = \frac{8}{\pi\alpha} \frac{1}{R_{\text{EP}}^1} \langle \sin(\Psi_{\text{EP}}^1 - \phi_p^*) \rangle$$

(recall)

¹ $\frac{dN}{d\Delta\phi_p^*} = p_0(1 + 2p_1 \sin(\Delta\phi_p^*) + 2p_2 \cos(\Delta\phi_p^*) + 2p_3 \sin(2\Delta\phi_p^*) + 2p_4 \cos(2\Delta\phi_p^*) + \dots)$



Results (previous)



$$P_\Lambda = \frac{8}{\pi\alpha_\Lambda} \frac{p_1}{R_{EP}^1}$$

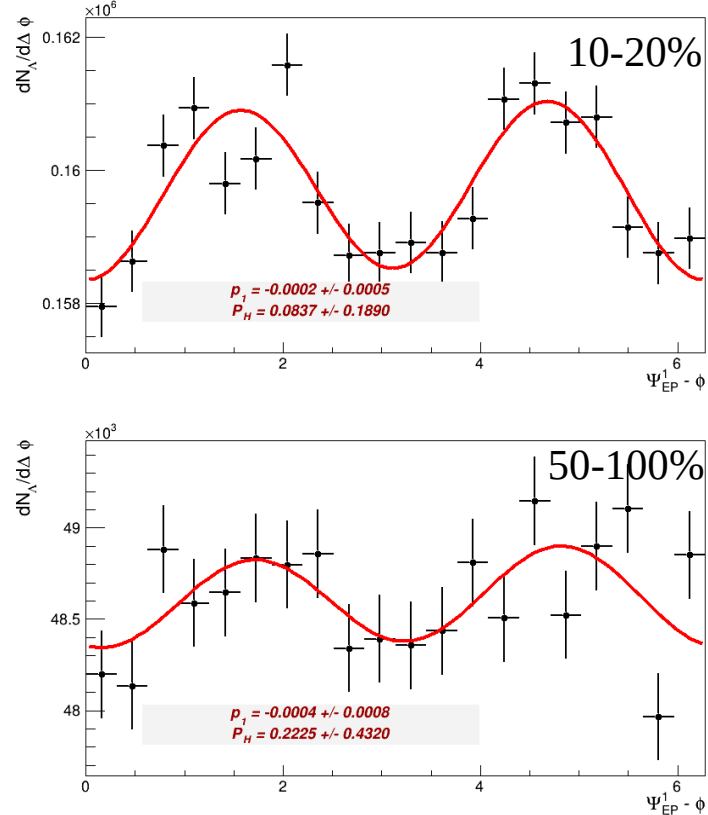
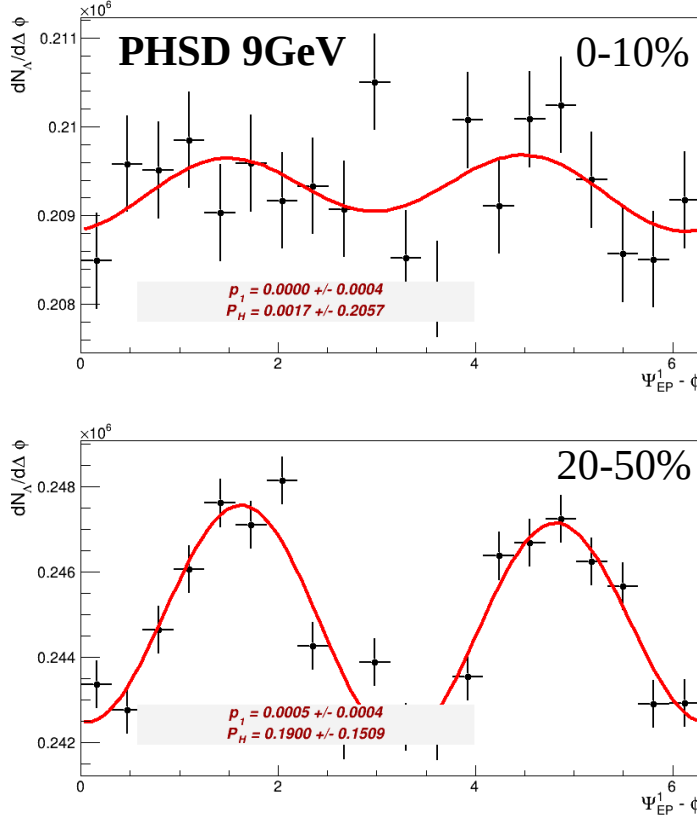
$$\alpha_\Lambda \simeq 0.732$$

	20-50%
N_Λ	$3.3 * 10^5$
p_0	$(1.6 +/- 3.3) * 10^4$
$p_1/10^{-4}$	$33.02 +/- 14.01$
$p_2/10^{-4}$	$44.03 +/- 13.93$
$p_3/10^{-4}$	$-3.26 +/- 13.95$
$p_4/10^{-4}$	$-52.39 +/- 14.00$

p_1 and p_2 are of the same magnitude order!

$$\frac{dN}{d\Delta\phi_p^*} = p_0(1 + 2p_1 \sin(\Delta\phi_p^*) + 2p_2 \cos(\Delta\phi_p^*) + 2p_3 \sin(2\Delta\phi_p^*) + 2p_4 \cos(2\Delta\phi_p^*) + \dots)$$

Results (new)



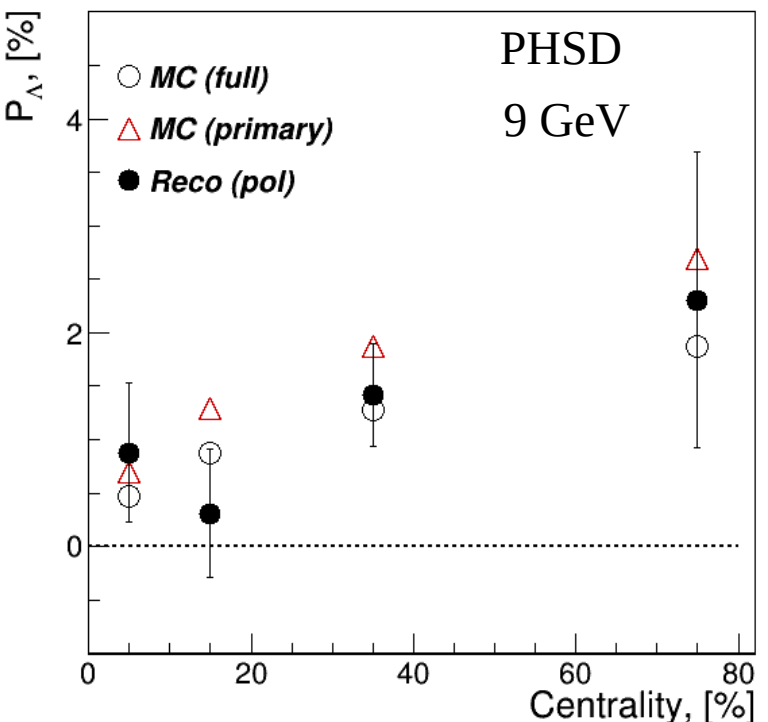
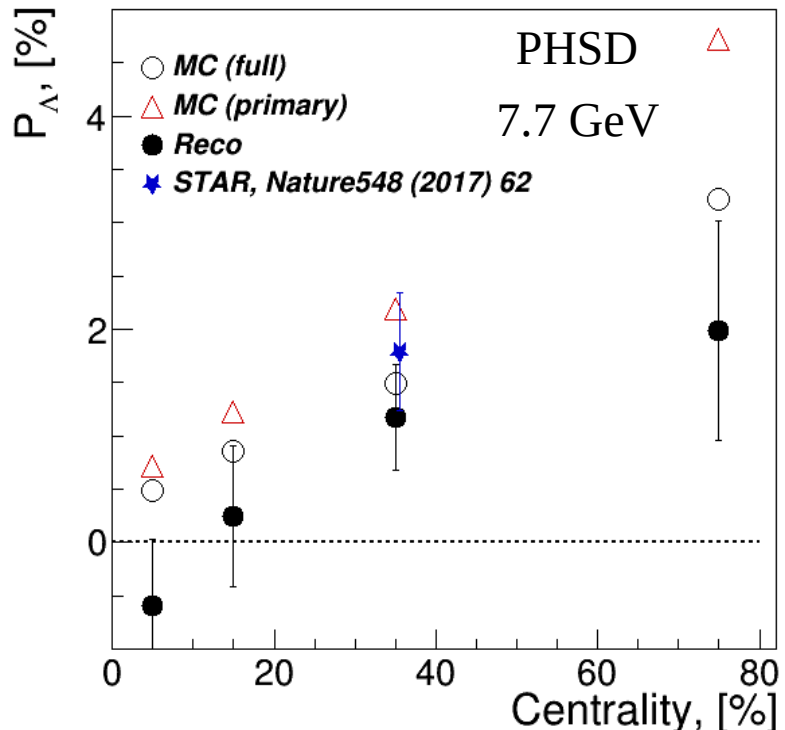
$$P_\Lambda = \frac{8}{\pi \alpha_\Lambda} \frac{p_1}{R_{EP}^1}$$

$$\alpha_\Lambda \simeq 0.732$$

	20-50%
N_Λ	$4.9 * 10^6$
p_0	$(2.5 \pm 1.3) * 10^5$
$p_1/10^{-4}$	4.57 ± 3.63
$p_2/10^{-4}$	4.39 ± 4.61
$p_3/10^{-4}$	-7.62 ± 3.62
$p_4/10^{-4}$	-51.52 ± 3.62

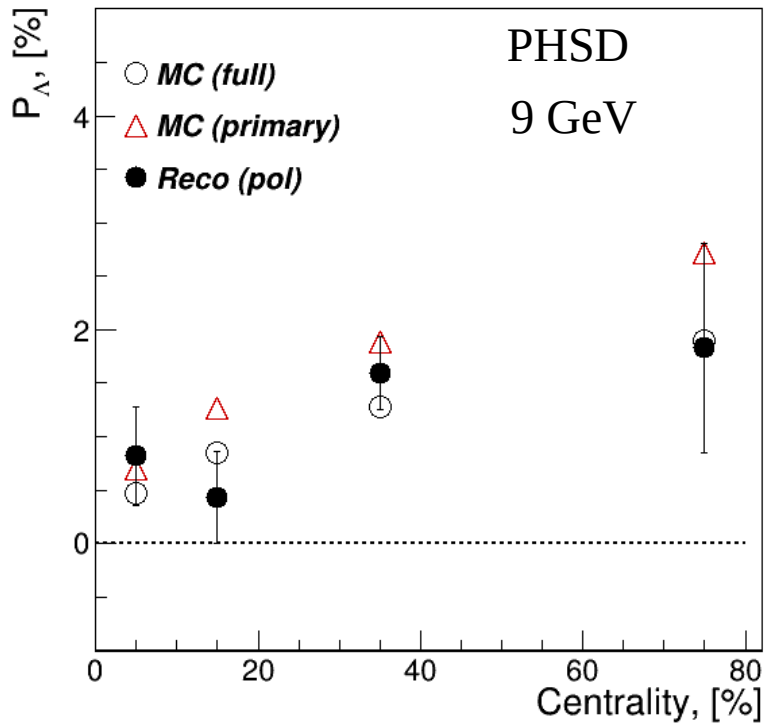
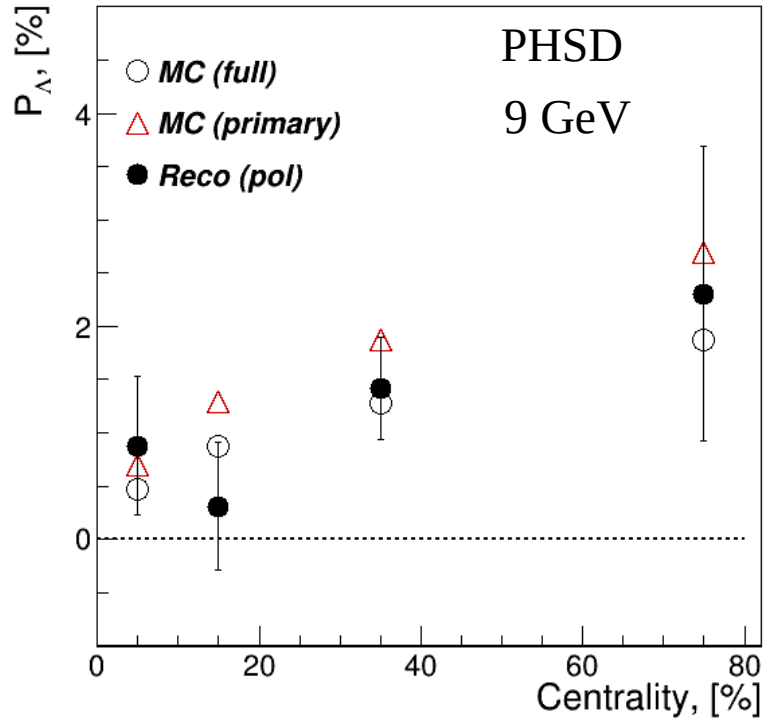
$$\frac{dN}{d\Delta\phi_p^*} = p_0(1 + 2p_1 \sin(\Delta\phi_p^*) + 2p_2 \cos(\Delta\phi_p^*) + 2p_3 \sin(2\Delta\phi_p^*) + 2p_4 \cos(2\Delta\phi_p^*) + \dots)$$

Results



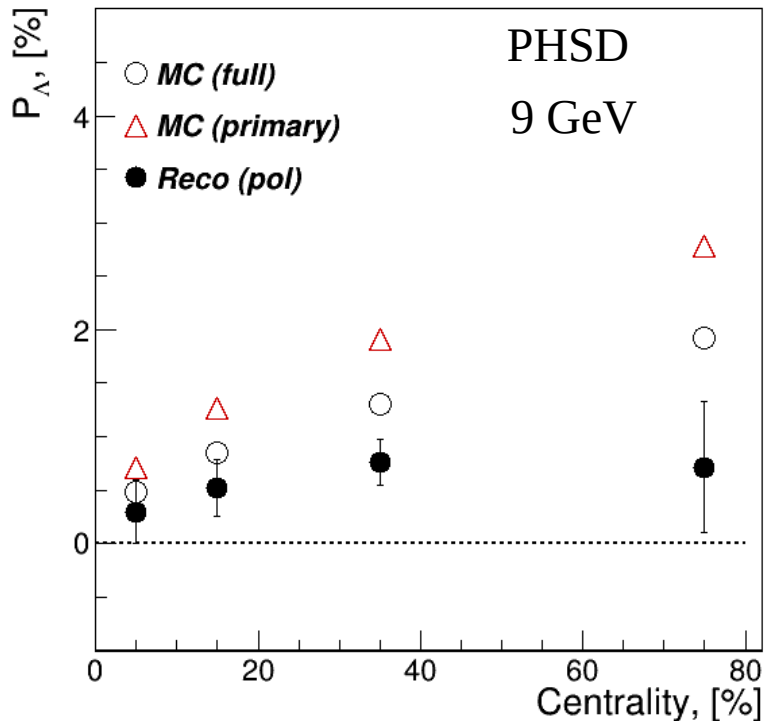
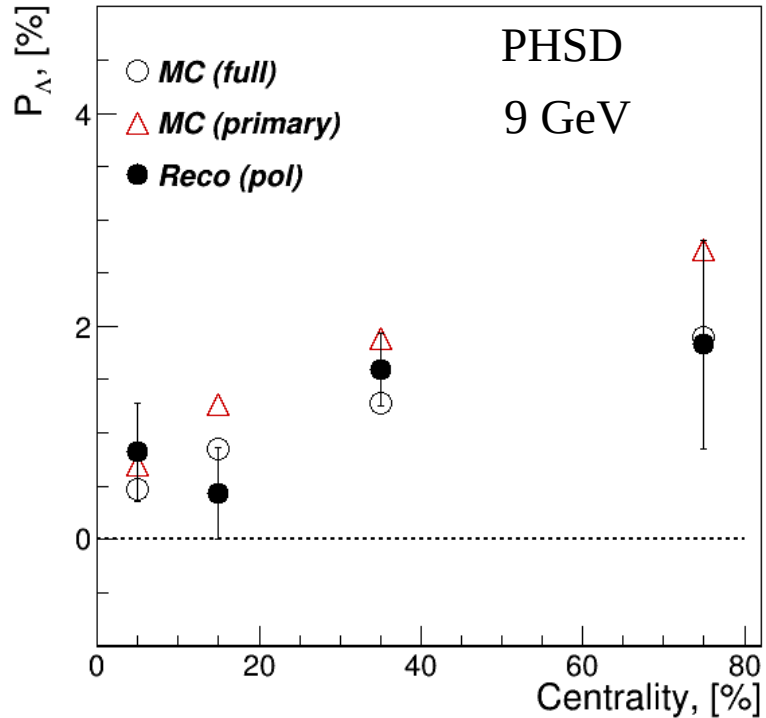
- (left) Previous result (PHSD ~1M events, @ 7.7 GeV)
- (right) New result with ~1M events, PHSD @ 9 GeV
- The results seem similar, but ...

Results



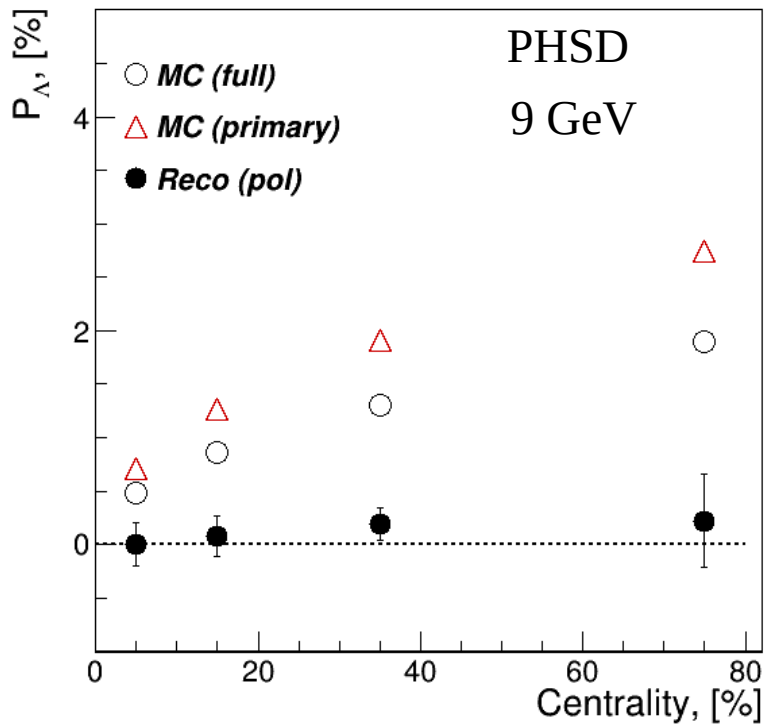
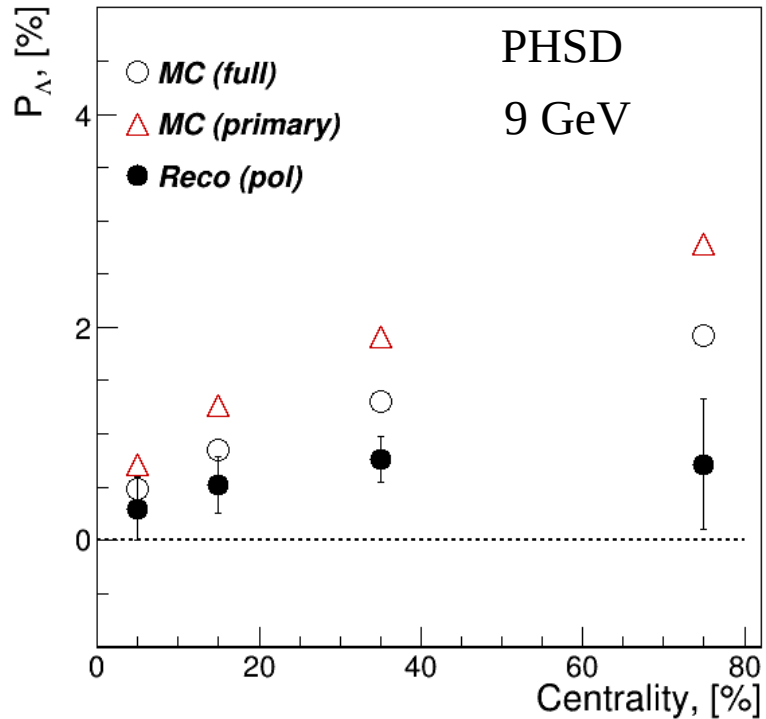
- (left) PHSD @ 9 GeV, ~1M events
- (right) PHSD @ 9 GeV, ~2M events
- When we increase statistics, the picture starts to change

Results



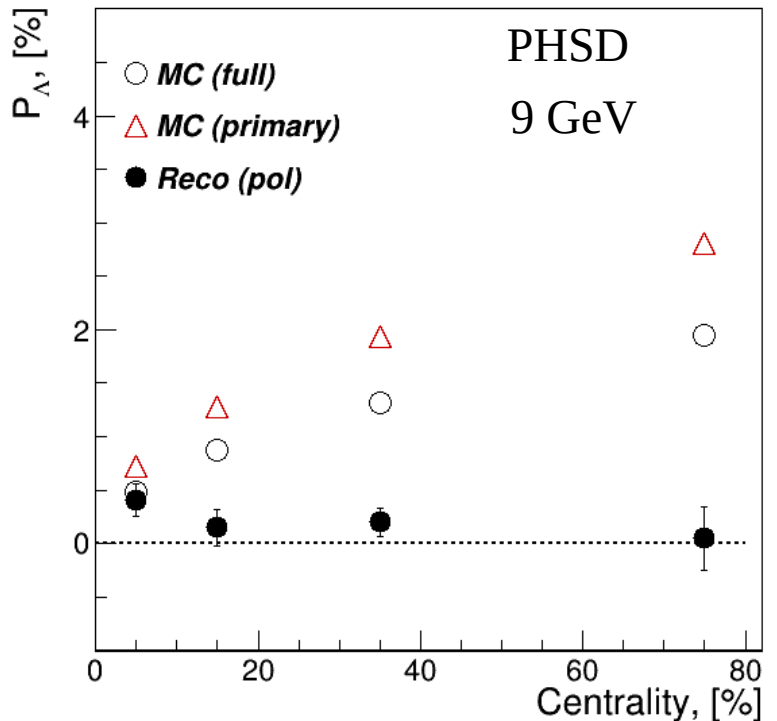
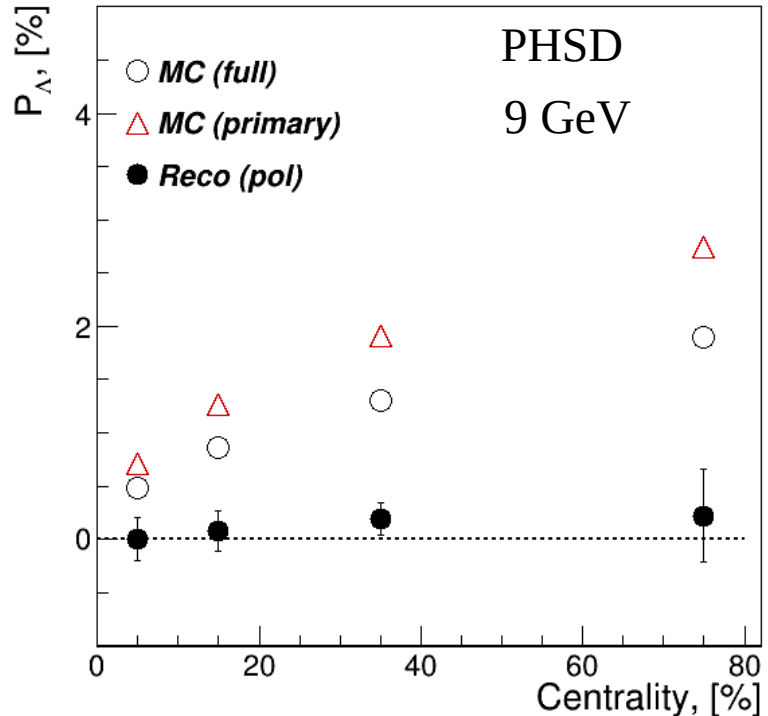
- (left) PHSD @ 9 GeV, ~2M events
- (right) PHSD @ 9 GeV, ~5M events
- Not only the errors are decreasing, but the value of polarization

Results



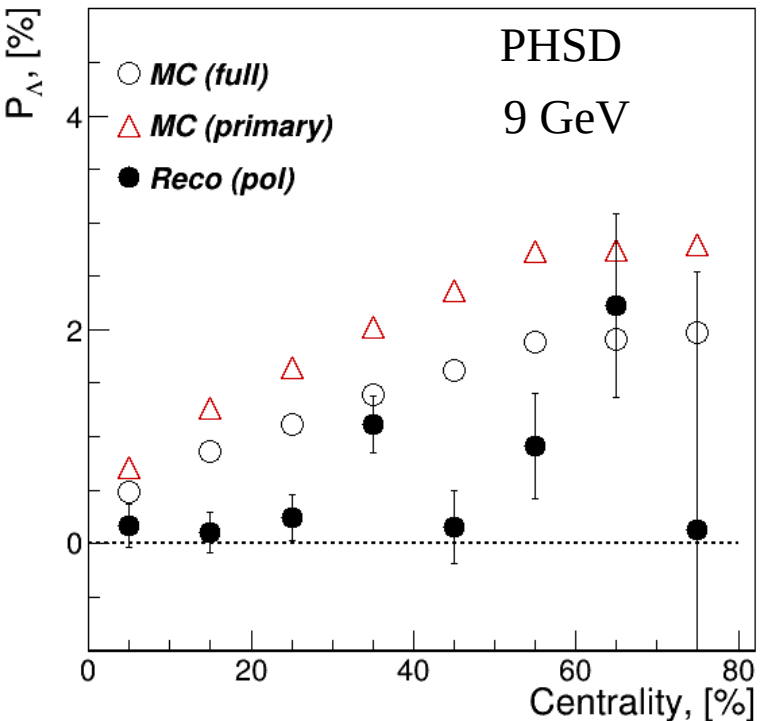
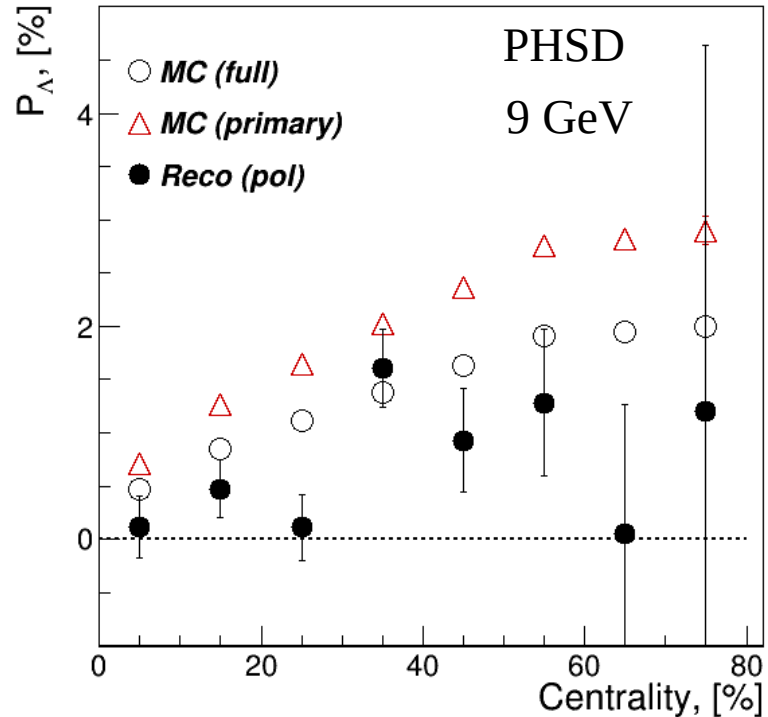
- (left) PHSD @ 9 GeV, ~5M events
- (right) PHSD @ 9 GeV, ~10M events
- Not only the errors are decreasing, but the value of polarization
- For the full sample, the reconstructed value is consistent with 0

Results



- (left) PHSD @ 9 GeV, ~10M events, using $\Delta\phi_p^* = \Psi_{EP}^1 - \phi_p^*$
- (right) PHSD @ 9 GeV, ~10M events, using $\Delta\phi_p^* = \Psi_{RP} - \phi_p^*$

Results



- (left) PHSD @ 9 GeV, ~5M events
- (right) PHSD @ 9 GeV, ~10M events
- Not only the errors are decreasing, but the value of polarization
- For the full sample, the reconstructed value is consistent with 0

Overview of statistics



	0-10%	10-20%	20-30%	30-40%	40-50%	50-60%	60-70%	70-80%	80-90%	90-100%
N _{events}	$1.3* 10^6$	$1.4* 10^6$	$1.4* 10^6$	$1.4* 10^6$	$1.4* 10^6$	$1.5* 10^6$	$1.2* 10^6$	$3.7* 10^5$	$7.5* 10^4$	$1.8* 10^3$
N _{Λ}	$4.4* 10^6$	$3.3* 10^6$	$2.4* 10^6$	$1.6* 10^6$	$1.0* 10^6$	$0.6* 10^6$	$0.3* 10^6$	$0.5* 10^5$	-	-

PHSD @9 GeV

	0-10%	10-20%	20-50%	50-100%
N _{events}	$1.3* 10^6$	$1.4* 10^6$	$4.2* 10^6$	$3.0* 10^6$
N _{Λ} (full)	$4.4* 10^6$	$3.3* 10^6$	$4.9* 10^6$	$1.0* 10^6$
N _{Λ} (5M)	$2.1* 10^6$	$1.6* 10^6$	$2.4* 10^6$	$0.5* 10^6$

PHSD @7.7 GeV

	20-50%
N _{events}	$2.9* 10^6$
N _{Λ}	$3.3* 10^5$

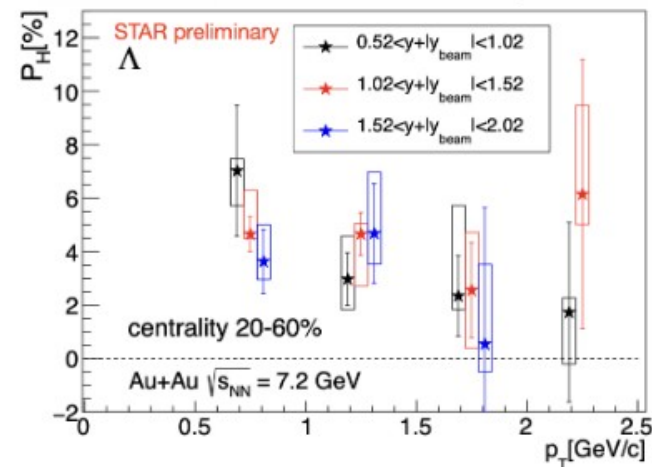
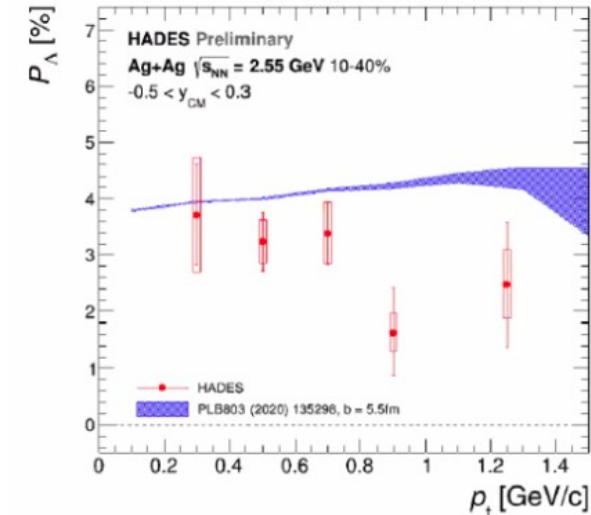
HADES

Au-Au @1.23 GeV
Ag-Ag @1.58 AGeV

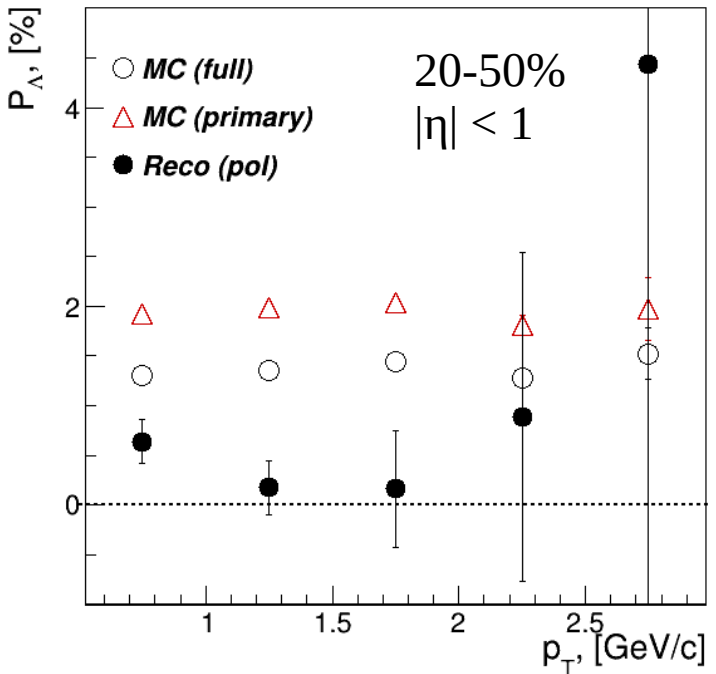
	10-40%
N _{Λ} (Au)	$1.5* 10^5$
N _{Λ} (Ag)	$1.1* 10^6$

Results

Transverse momentum dependence



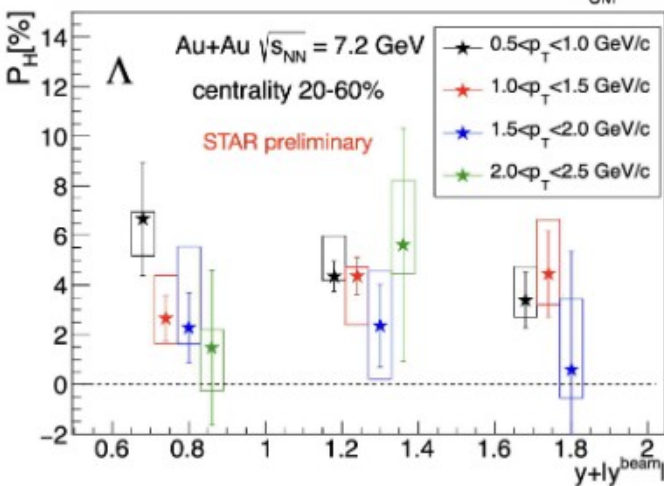
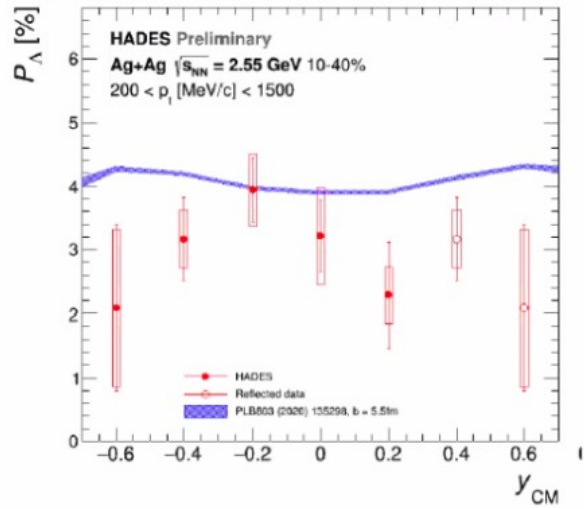
PHSD, BiBi @9 GeV



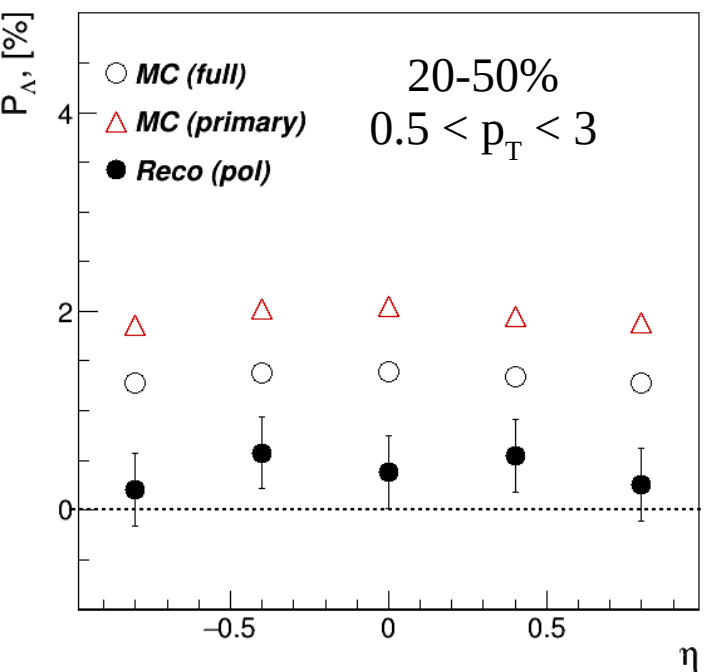
- Rapidity and transverse momentum dependences of global polarization of Lambda
 - STAR collaboration, SQM2021 (e-Print: 2108.10012)
 - HADES collaboration, SQM2021
- No significant y and p_T dependence within uncertainties

Results

Rapidity dependence

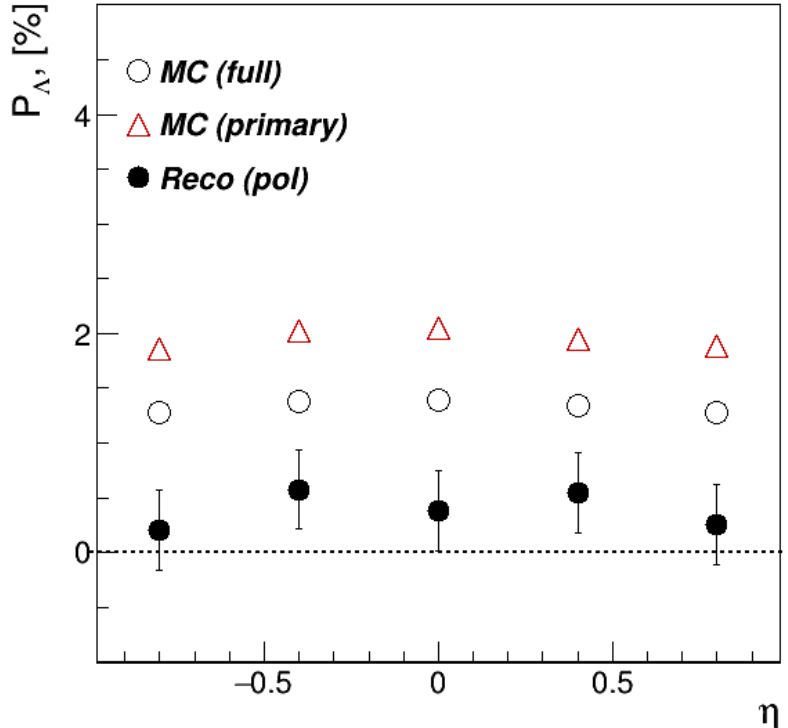
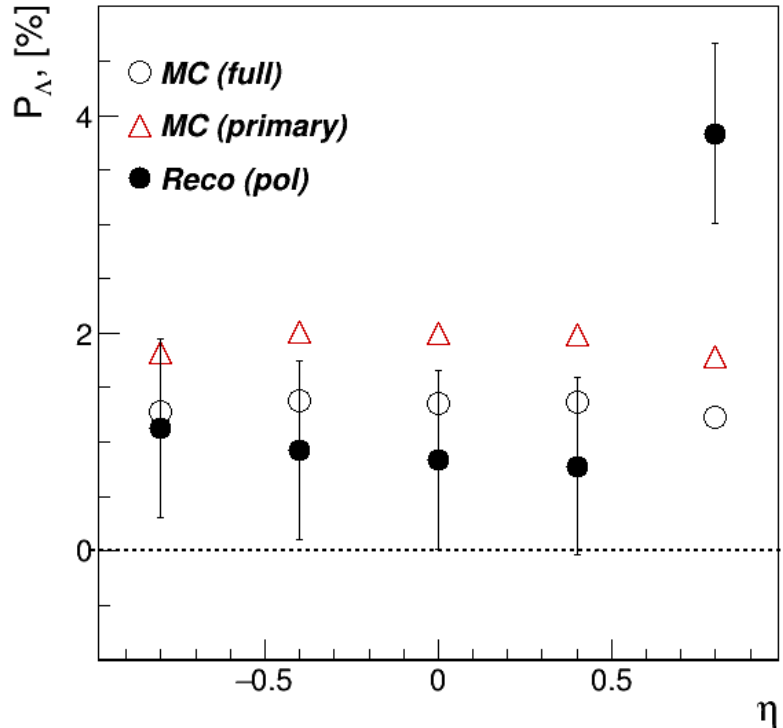


PHSD, BiBi @9 GeV



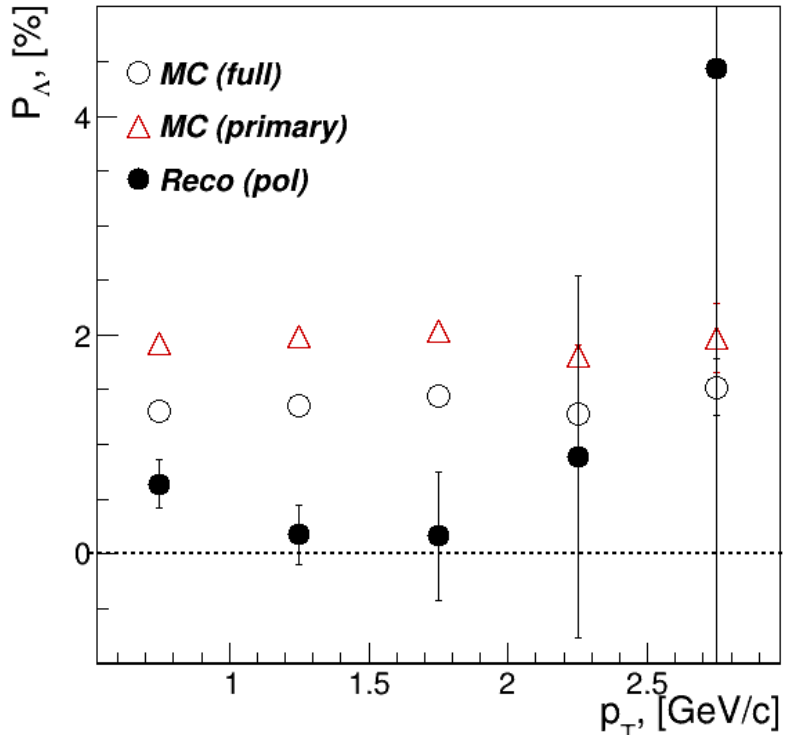
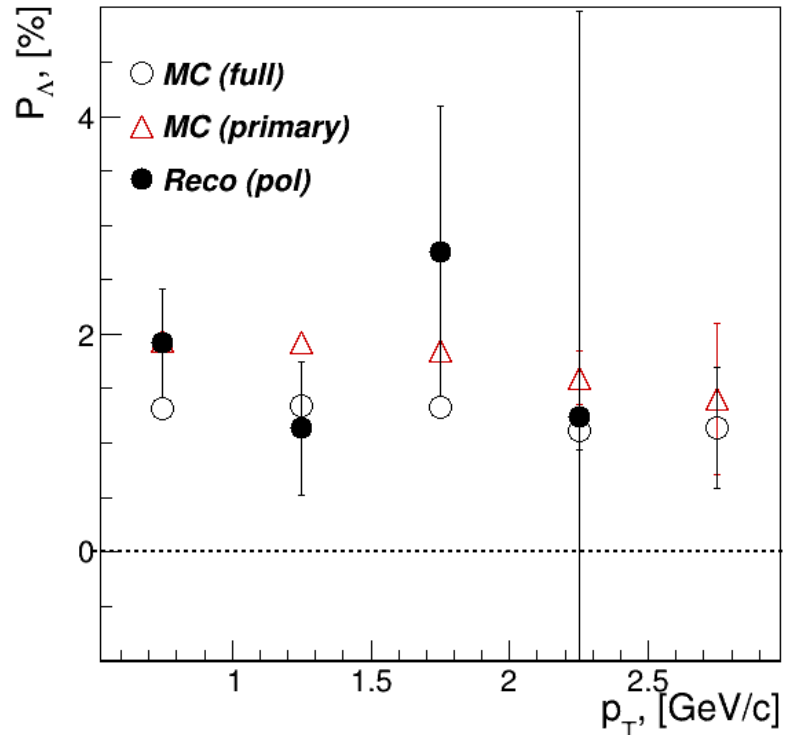
- Rapidity and transverse momentum dependences of global polarization of Lambda
 - STAR collaboration, SQM2021 (e-Print: 2108.10012)
 - HADES collaboration, SQM2021
- No significant y and p_T dependence within uncertainties

Results



- (left) PHSD @ 9 GeV, ~2M events
- (right) PHSD @ 9 GeV, ~10M events

Results



- (left) PHSD @ 9 GeV, ~2M events
- (right) PHSD @ 9 GeV, ~10M events

Conclusions

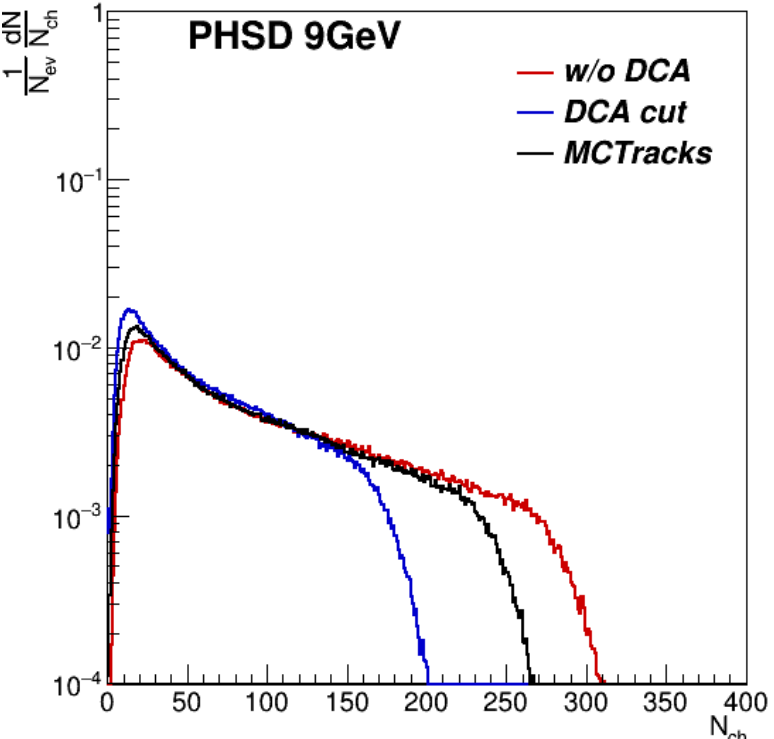
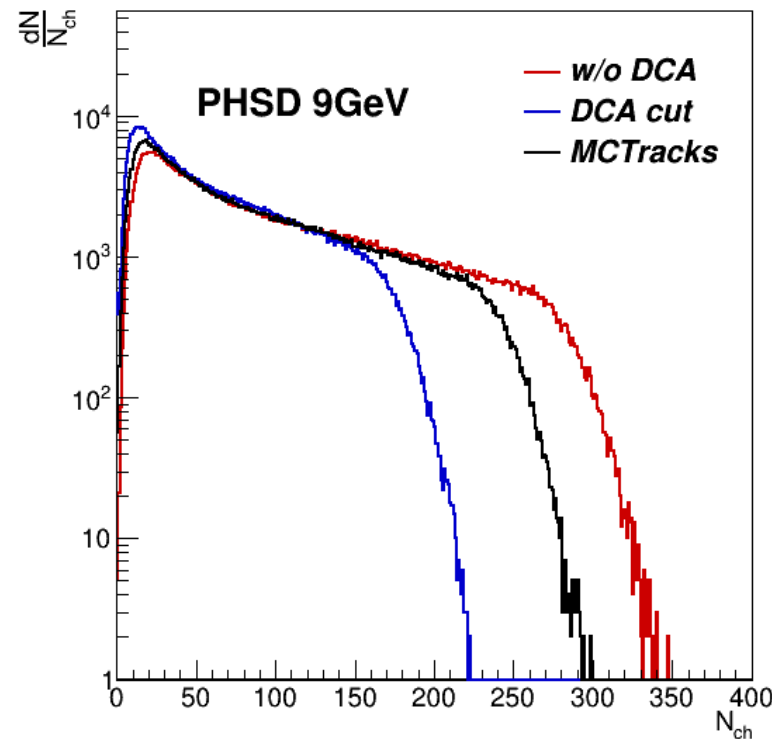


- Feasibility study of the global polarization measurement with PHSD
 - Sample with increased statistics: Bi-Bi @ 9GeV, 10M MB events, b [0,12]fm
 - Official production (request 23)
- Compared with our previous results from the testing sample (Au-Au @ 7.7GeV, 1.4M MB events, b [0,16]fm)
 - Better results with centrality and EP resolution determination
 - Unexpected behaviour of extracted global polarization values
- Outlook
 - Does the method become inapplicable/should be corrected?
 - Is the picture the same with the second method?



Thank you for your attention!

Back Up: Multiplicity in TPC



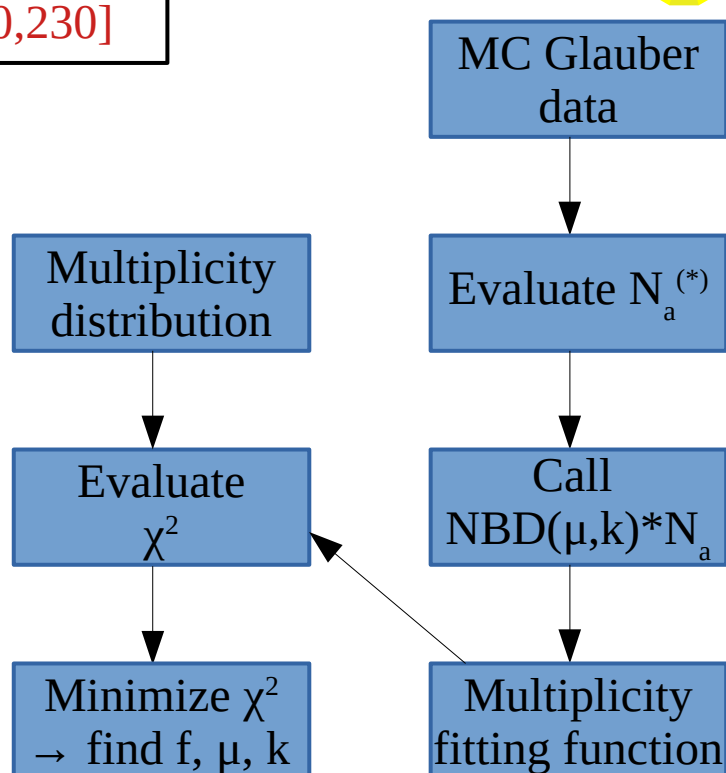
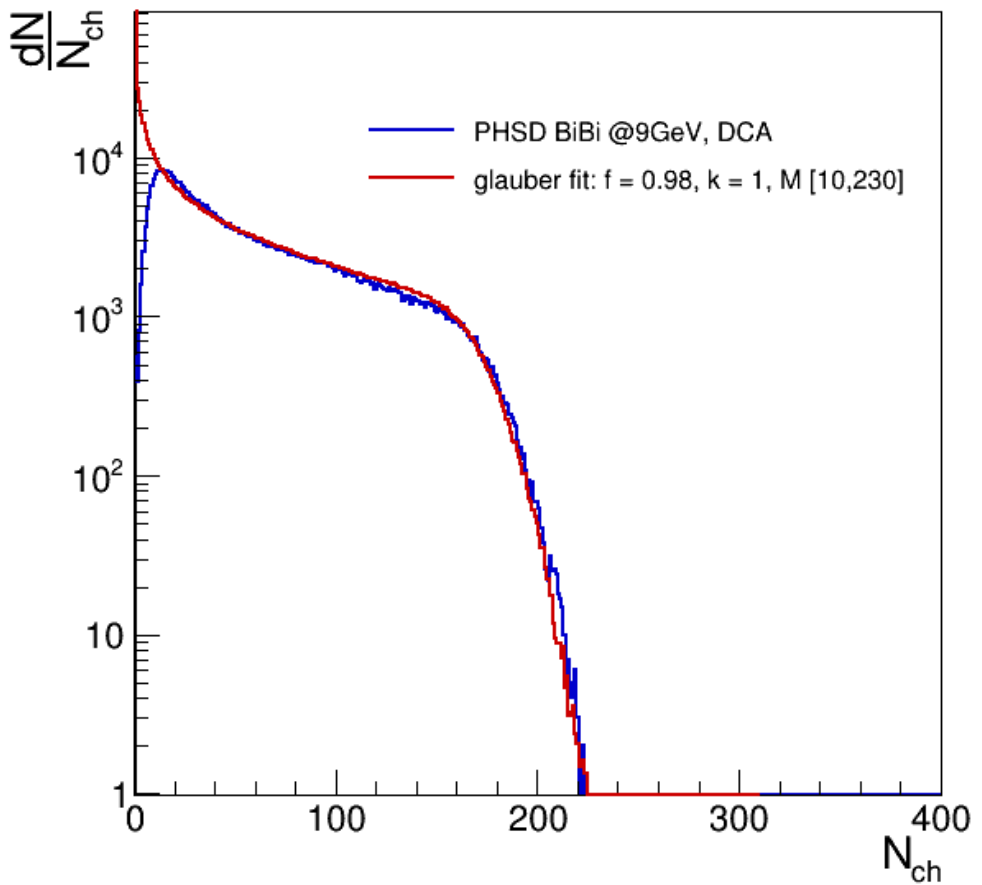
- MC-Glauber based centrality framework¹
- Selection criteria:
 - > 500k events
 - > $|\eta| < 0.5$
 - > $|p_T| > 0.15$ GeV
 - > $N_{\text{hits}} > 16$
 - > $|DCA| < 0.5$ cm (optional)
 - > 10%-centrality bins

¹ P. Parfenov et al, NRNU MEPhI for the MPD collaboration
(<https://github.com/FlowNICA/CentralityFramework>)

Back Up: Centrality determination

$$f = 0.98, \mu = 0.43, k = 1, \chi^2 = 15.32 \pm 0.36$$

DCA cut, M [10,230]

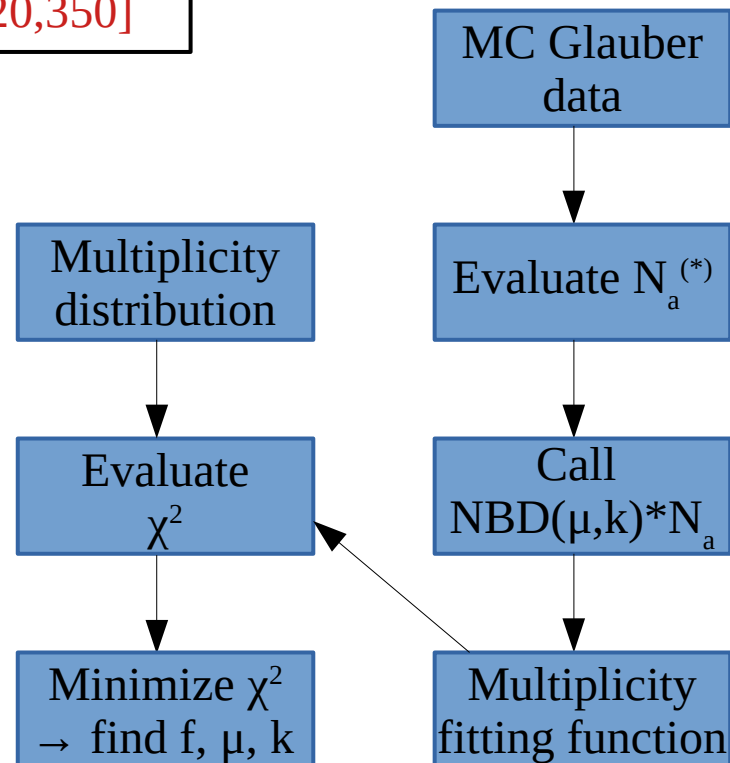
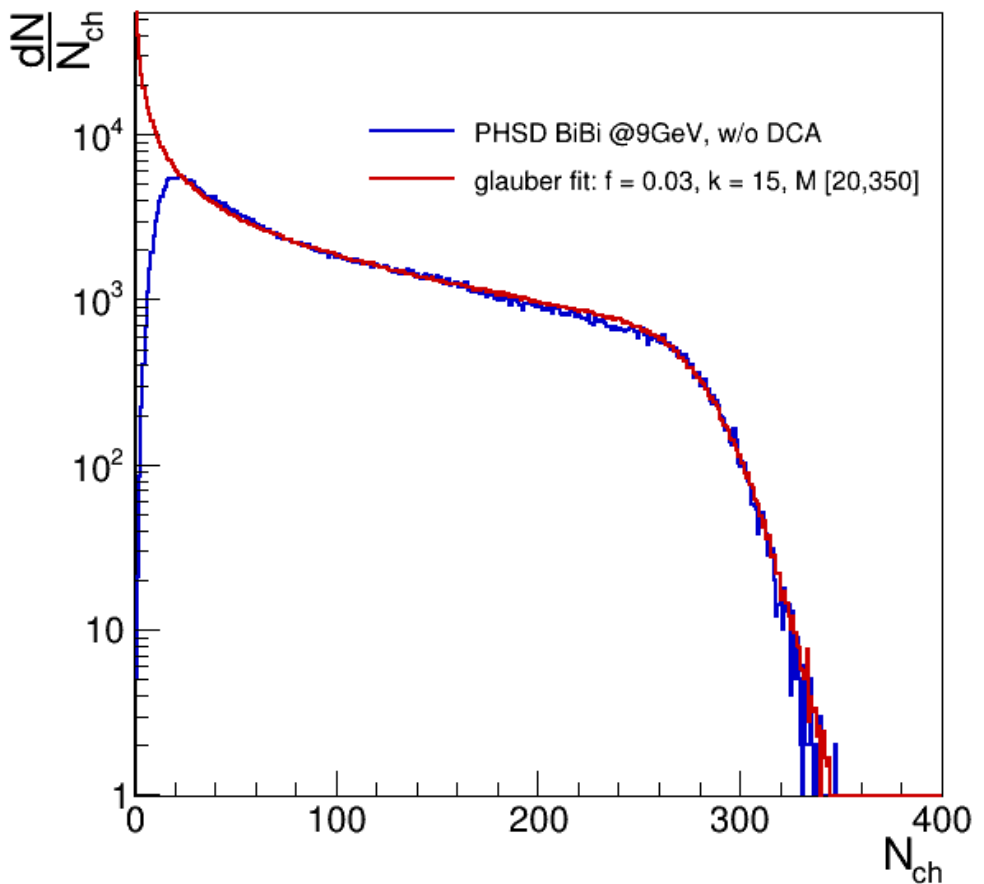


$${}^{(*)}N_a = fN_{part} + (1 - f)N_{coll}$$

Back Up: Centrality determination

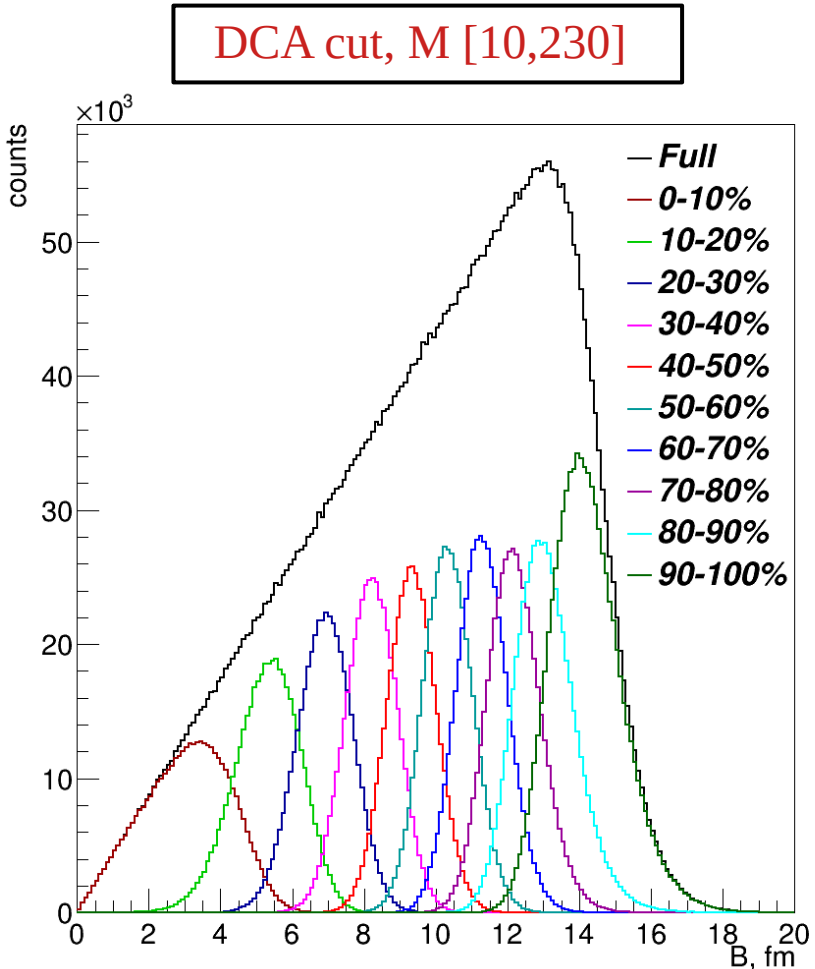
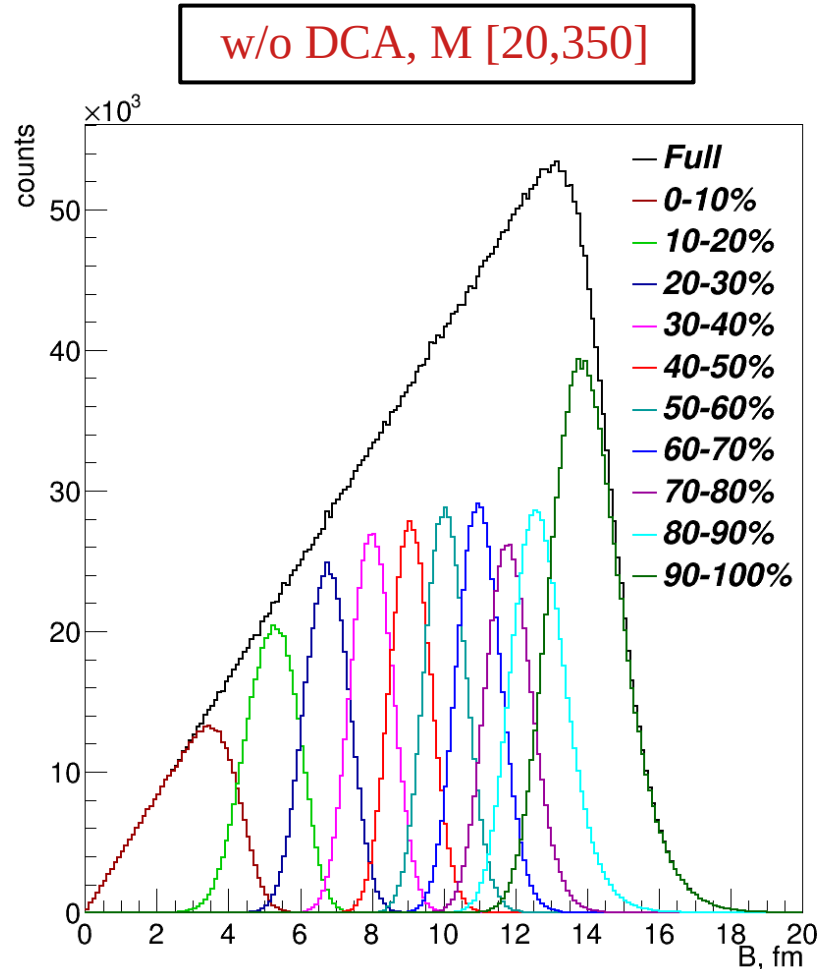
$$f = 0.03, \mu = 0.31, k = 15, \chi^2 = 3.65 \pm 0.11$$

w/o DCA, M [20,350]



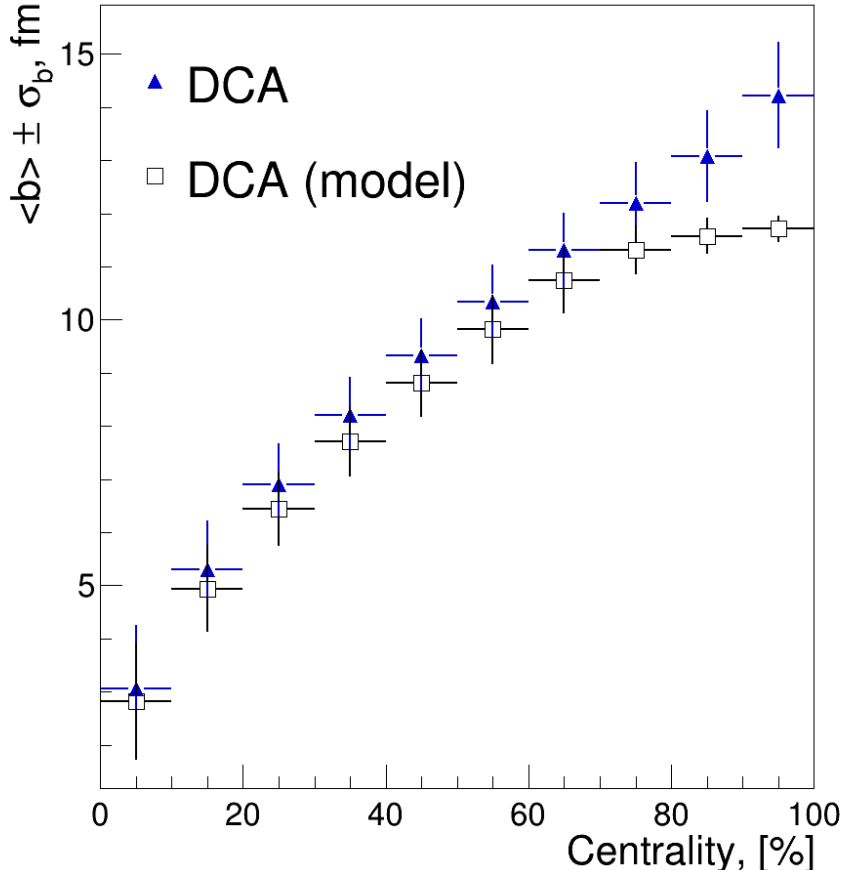
$${}^{(*)}N_a = fN_{\text{part}} + (1 - f)N_{\text{coll}}$$

Back Up: Centrality determination

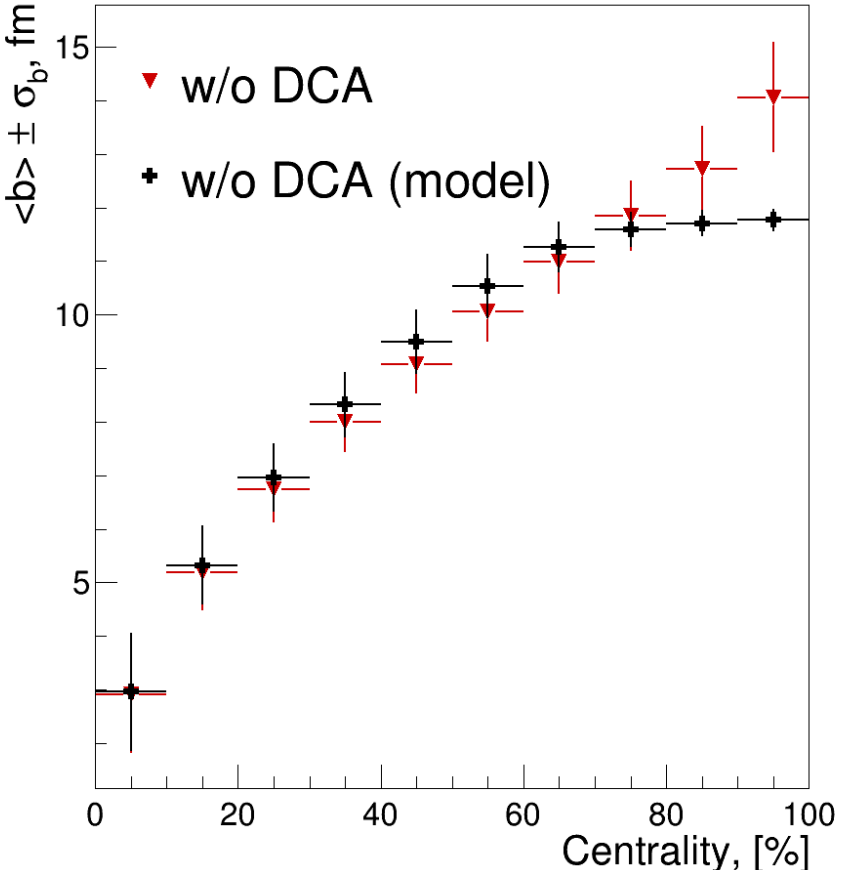


Back Up: Average impact parameter

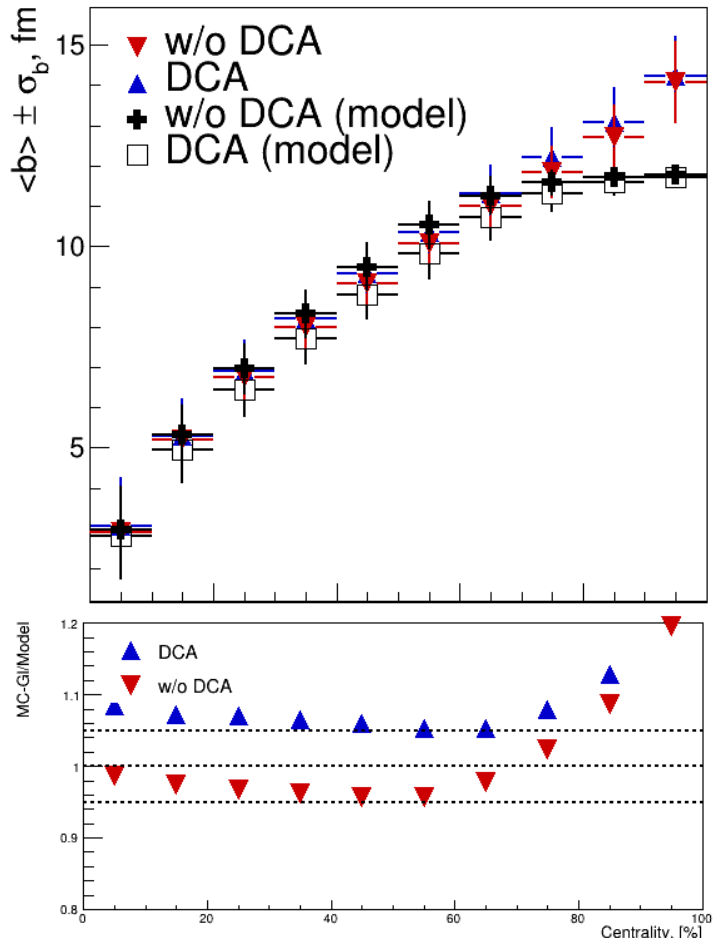
DCA cut, M [10,230]



w/o DCA, M [20,350]



Back Up: Average impact parameter



Back Up: Parameters from centrality framework



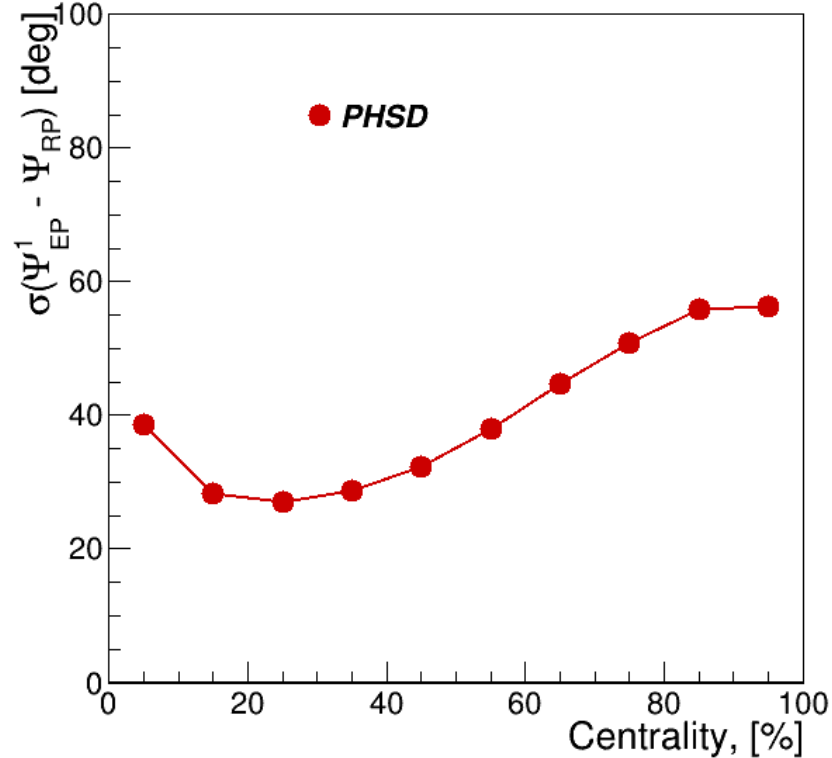
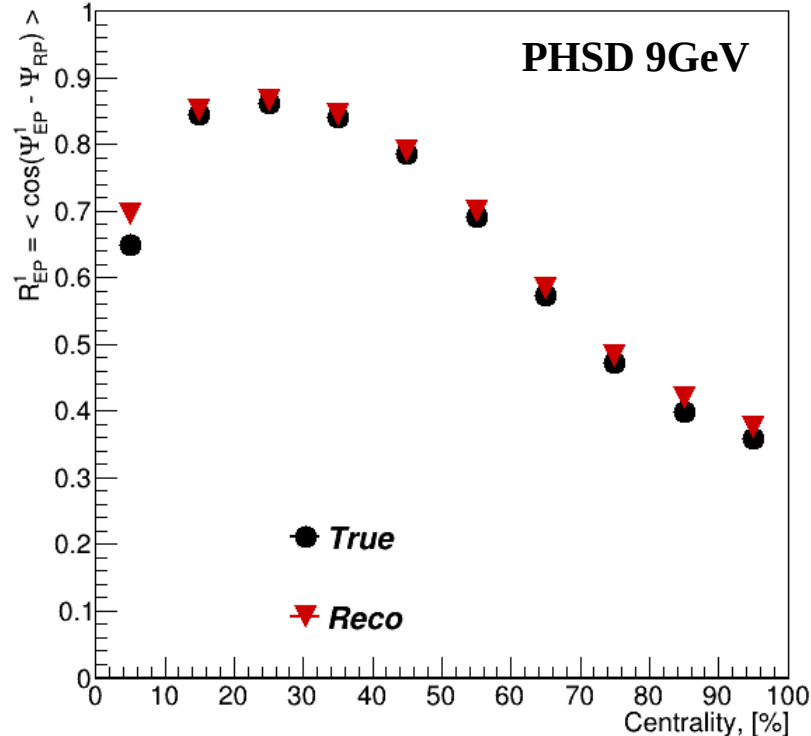
Centrality, %	N_{ch}^{min}	N_{ch}^{max}	$\langle b \rangle$, fm	RMS	b_{min} , fm	b_{max} , fm	$\langle N_{part} \rangle$	RMS	N_{part}^{min}	N_{part}^{max}	$\langle N_{coll} \rangle$	RMS	N_{coll}^{min}	N_{coll}^{max}
0 - 10	127	232	3.06	1.21	1.54	4.28	336.78	37.71	292.83	387.52	748.61	113.62	627.36	890.99
10 - 20	94	127	5.30	0.92	4.28	6.16	254.64	36.00	219.87	292.83	524.17	101.49	434.17	627.36
20 - 30	69	94	6.90	0.78	6.16	7.58	189.45	30.00	162.66	219.87	357.94	79.26	293.21	434.17
30 - 40	49	69	8.20	0.72	7.58	8.78	138.34	25.24	117.29	162.66	237.63	61.37	191.21	293.21
40 - 50	34	49	9.33	0.69	8.78	9.85	98.20	20.73	81.42	117.29	151.55	45.65	118.68	191.21
50 - 60	22	34	10.35	0.69	9.85	10.84	66.94	17.09	53.69	81.42	91.64	33.18	68.90	118.68
60 - 70	13	22	11.31	0.71	10.84	11.75	42.59	13.44	33.20	53.69	50.91	22.41	36.82	68.90
70 - 80	7	13	12.20	0.76	11.75	12.63	25.22	9.95	18.92	33.20	25.98	13.88	18.04	36.82
80 - 90	3	7	13.08	0.87	12.63	13.61	13.68	6.99	9.16	18.92	12.18	8.06	7.69	18.04
90 - 100	1	2	14.22	1.00	13.61	14.97	5.13	3.36	1.02	9.16	3.77	3.13	-0.60	7.69

↑ DCA cut, M [10,230]

w/o DCA, M [20,350] ↓

Centrality, %	N_{ch}^{min}	N_{ch}^{max}	$\langle b \rangle$, fm	RMS	b_{min} , fm	b_{max} , fm	$\langle N_{part} \rangle$	RMS	N_{part}^{min}	N_{part}^{max}	$\langle N_{coll} \rangle$	RMS	N_{coll}^{min}	N_{coll}^{max}
0 - 10	193	355	2.92	1.09	1.30	4.18	341.13	33.89	297.02	392.86	767.45	95.49	641.69	916.61
10 - 20	135	193	5.19	0.72	4.18	6.03	259.03	29.90	225.32	297.02	535.50	70.25	447.39	641.69
20 - 30	93	135	6.74	0.61	6.03	7.39	195.95	25.17	169.74	225.32	372.76	54.10	308.16	447.39
30 - 40	62	93	8.00	0.57	7.39	8.54	146.01	21.34	125.37	169.74	253.46	42.14	206.93	308.16
40 - 50	40	62	9.08	0.56	8.54	9.59	106.45	17.91	89.62	125.37	166.85	32.22	133.08	206.93
50 - 60	24	40	10.06	0.57	9.59	10.55	74.98	15.09	61.30	89.62	104.73	24.64	80.42	133.08
60 - 70	13	24	11.00	0.61	10.55	11.41	49.57	12.41	39.76	61.30	60.45	18.15	45.09	80.42
70 - 80	7	13	11.85	0.66	11.41	12.26	31.20	9.73	24.04	39.76	33.01	12.43	23.55	45.09
80 - 90	3	7	12.72	0.81	12.26	13.32	17.82	7.89	12.00	24.04	16.39	8.72	10.53	23.55
90 - 100	1	2	14.06	1.03	13.32	15.03	6.15	4.27	-0.56	12.00	4.61	3.86	-2.99	10.53

Back Up: Event plane determination



- Event plane and its resolution determined using FHCAL
- Checked via 2 methods